The mechanism of malate-induced stomatal closure in *Arabidopsis thaliana*

2022, March

Yoshiharu Mimata

Graduate School of Environmental and Life Science

(Doctor’s Course)

OKAYAMA UNIVERSITY

Contents

LIST OF FIGURES

CHAPTER 1

General Introduction

1.1. Stomata

Higher plants have numerous air vents called stomata (singular “stoma”) in the epidermis of wax-covered impervious leaves and exchange gas through stomata, such as O_2 used in respiration, CO_2 used in photosynthesis and H_2O for transpiration. The plants control the rate of gas exchange by opening and closing their stomata and thus adapt to changes in environmental factors including water potential, CO_2 concentration, and light intensity (Hetherington & Woodward, 2003). Stomata are formed by pairs of guard cells and stomatal movements are driven by changes in turgor pressure of the guard cells (Schroeder et al., 2001). When guard cells expand due to the increase in turgor pressure, stomata open; when guard cells contract due to the decrease in turgor pressure, stomata close (Fig. 1.1). Guard cells have diverse signaling systems that regulate turgor pressure in response to stimuli such as phytohormones, CO_2, ozone, drought, relative humidity, light and microbe invasion (Schroeder et al., 2001; Shimazaki, et al., 2007; Melotto et al., 2008; Hedrich, 2012; Murata et al., 2015). Among them, the signaling mechanism by which a phytohormone abscisic acid (ABA) induces stomatal closure has been well studied.

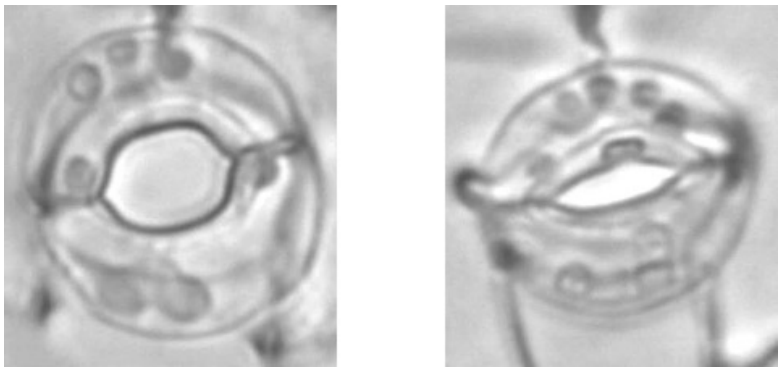

Open Stoma Closed Stoma

Fig 1.1. Arabidopsis stomata

1.2. Abscisic acid-induced stomatal closure

Phytohormones are biosynthetic signal molecules and control plant growth and development. ABA is a well-studied phytohormone which induces stomatal closure. ABA is synthesized under drought stress and contributes to drought tolerance. ABA activates protein kinase such as SUCROSE NON-FERMENTING1-RELATED PROTEIN KINASE 2s (SnRK2s) and cytosolic calcium sensor kinases CALCIUM-DEPENDENT PROTEIN KINASEs (CPKs) through signal transduction and these kinases further activates two types of anion channels expressed in the plasma membrane, slow-type (S-type) anion channels and rapid-type (R-type) anion channels (Schroeder and Hagiwara, 1989; Hedrich et al., 1990). These anion channels mediate efflux of anions such as Cl^- and malate from guard cells, which results in decrease in turgor pressure and promoting stomatal closure to minimize water loss (Keller et al., 1989; Schroeder & Hagiwara, 1989; Linder & Raschke, 1992; Schroeder & Keller, 1992). ABA also triggers recruitment of second messengers including reactive oxygen species (ROS) and Ca^{2+}, which involves in activation of these anion channels.

1.3. The role of malate in stomatal movements

Malate is an essential organic acid that is biosynthesized by all living organisms. In plants, malate has special important roles. From a biochemical point of view, malate is not only an intermediate in the TCA cycle but also a CO_2 fixation product in photosynthesis and malate–starch interconversion (Daloso et al., 2017). From a physiological point of view, malate is secreted from roots in response to Al^{3+} and reduces Al^{3+} stress by chelation (Delhaize and Ryan, 1995). Furthermore, malate is also secreted from guard cells and regulates stomatal movements (Hedrich et al., 1993).

Malate represents a major organic osmolyte in guard cells. Malate accounts for most of CO_2 fixation products and accumulates in guard cells under light (Allaway, 1973;

Dittrich and Raschke, 1977). Malate is secreted from guard cells and mesophyll cells in response to ABA or elevated CO_2 and the concentration of apoplastic malate increases to several mM (Van Kirk & Raschke, 1978b; Kondo & Maruta, 1987; Hedrich *et al.*, 1994; Gabriel & Kesselmeier, 1999). External application of malate to apoplast induced stomatal closure in a concentration-dependent manner (Hedrich *et al.*, 1994; Lee *et al.*, 2008; Araújo *et al.*, 2011), suggesting that malate regulates stomatal movements. It was subsequently shown that extracellular malate activates S-type anion channels and R-type anion channels (Hedrich & Marten, 1993; Raschke, 2003; Konrad & Hedrich, 2008; Wang & Blatt, 2011) and that stomatal closure induced by malate is completely abolished by the blockage of anion channels (Schroeder et al., 1993). These results indicate that malate induces stomatal closure through the activation of anion channels. Importantly, pharmacological results also revealed that malate-induced stomatal closure are abolished by the inhibition of protein kinase (Schmidt et al., 1995). Therefore, it is speculated that malate, like ABA, regulates signal transduction of stomatal closure. Furthermore, the disruption of a malate exporter of guard-cell plasma membrane impaired ABA- and elevated CO_2-induced stomatal closure (Meyer et al., 2010; Sasaki et al., 2010). This finding increases the validity of the speculation and emphasize the importance of extracellular malate in stomatal closure. However, the mechanism by which malate induce stomatal closure remains unclear.

1.4. Anion channels in guard cells

Two types of anion channels are identified as regulators of stomatal closure in the plasma membrane of guard cells. One is an S-type anion channel and the other is an R-type anion channel. In *A. thaliana* guard cells, SLOW ANION CHANNEL-ASSOCIATED1 (SLAC1) represents the S-type anion channel (Negi *et al.*, 2008; Vahisalu *et al.*, 2008; Geiger *et al.*, 2011) and ALUMINUM-ACTIVATED MALATE TRANSPORTER12

(ALMT12)/QUICK-ACTIVATING ANION CHANNEL1 (QUAC1) represents the R-type anion channel (Sasaki et al., 2010; Meyer et al., 2010). Since the disruption of either SLAC1 or ALMT12/QUAC1 impaired ABA- and elevated CO_2-induced stomatal closure (Negi *et al.*, 2008; Vahisalu *et al.*, 2008; Sasaki et al., 2010; Meyer et al., 2010), these anion channels are required for stomatal closure. These anion channels are activated by protein kinases *e.g.* SUCROSE NON-FERMENTING1-RELATED PROTEIN KINASEs (SnRKs), CALCIUM-DEPENDENT PROTEIN KINASEs (CPKs) and GUARD CELL HYDROGEN PEROXIDE-RESISTANT1 (GHR1) in response to stomatal closing stimuli (Mori *et al*., 2006; Brandt *et al.*, 2015; Sierla *et al*., 2018). Activated these anion channels mediate anion efflux from guard cells, which results in decrease in turgor pressure and promoting stomatal closure.

1.5. Second messengers in stomatal closure signaling

Reactive oxygen species (ROS) and Ca^{2+} function as universal second messengers in both animals and plants. In stomatal closure signaling, these second messengers transduce signals to ion channels of the plasma membrane. ROS, such as hydrogen peroxide, superoxide anion, hydroxyl radical and singlet oxygen, are literally “reactive” chemicals that are made from oxygen molecules and cause oxidative stress. Among phytohormones, ABA and methyl jasmonate induce NAD(P)H oxidases-catalyzed ROS production and salicylic acid induces peroxidases-catalyzed ROS production (Pei et al., 2000; Mori et al., 2001; Suhita et al., 2004). ROS activate plasma membrane Ca^{2+}-permeable channels and thereby increase cytosolic Ca^{2+} concentration in guard cells (Pei et al., 2000). The elevation in cytosolic Ca^{2+} concentration leads to activation of cytosolic calcium sensor kinases CALCIUM-DEPENDENT PROTEIN KINASEs (CPKs), which specifically phosphorylate S-type anion channels, leading to channel activation and finally stomatal closure (Mori et al., 2006).

1.6. Purpose of the study

To clarify the mechanism of malate-induced stomatal closure in *Arabidopsis thaliana*, the present study was set to achieve the following objectives:

- To identify components of malate singling in guard cells
- To elucidate the mechanism by which malate regulates the activity of anion channels of guard cells

CHAPTER 2

Extracellular malate induces stomatal closure *via* direct activation of guard-cell anion channel SLAC1 in *Arabidopsis thaliana*

2.1. Abstract

Previous studies reported that plants secrete malate from guard cells to apoplast under stress conditions and exogenous malate induces stomatal closure, suggesting that malate is considered as an extracellular chemical signal of stomatal closure. However, the molecular mechanism of malate-induced stomatal closure is not fully elucidated. I investigated responses of stomatal aperture and ion channels to malate. A treatment with malate induced stomatal closure in *Arabidopsis thaliana* wild-type plants but not in the mutants deficient in the anion channel gene *SLAC1.* Extracellular application of malate increased S-type anion currents in guard-cell protoplasts of wild-type plants but not in guard-cell protoplasts of the *slac1* mutant. Extracellular application of malate increased SLAC1-mediated S-type currents when SLAC1 was co-expressed with the protein kinases OST1 or CPK6, but not when SLAC1 was expressed alone in a heterologous expression system using *Xenopus* oocytes. In addition, extracellular rather than intracellular application of malate increased the S-type currents of constitutively active mutants of SLAC1, which have kinase-independent activities. The malate activation of SLAC1 was abrogated by mutation of E464 of SLAC1 at extracellular domain. These results indicate that extracellular malate directly activates SLAC1 in guard cells, resulting in stomatal closure.

2.2. Introduction

Deterioration of environments caused by global warming contributes to decreased crop productivity. Plants respond to changes in environmental factors such as water potential, CO_2 concentration, and light intensity by adjusting the aperture of stomatal pores, which are formed by pairs of guard cells in the epidermis of leaves, and thereby adapt to the detrimental conditions (Hetherington & Woodward, 2003). Stomatal movements are accompanied by transports of osmolytes across the plasma membrane of guard cells (Schroeder *et al.*, 2001; Hedrich, 2012). Malate is one of the vital osmolytes for stomatal movements (Allaway, 1973; Dittrich & Raschke, 1977; Outlaw & Lowry, 1977; Van Kirk & Raschke, 1978a; Raschke & Schnabl, 1978; Fernie & Martinoia, 2009).

Malate is released from guard cells to apoplast through malate transporters such as ALUMINUM-ACTIVATED MALATE TRANSPORTERs (ALMTs) (Meyer *et al.*, 2010; Sasaki *et al.*, 2010). The concentration of apoplastic malate can increase up to several mM in response to a phytohormone abscisic acid (ABA) or elevated CO_2 (Van Kirk & Raschke, 1978b; Kondo & Maruta, 1987; Hedrich *et al.*, 1994; Gabriel & Kesselmeier, 1999).

Malate is considered to function not only as an osmolyte but also as a signaling component in the stomatal movement. The mutation of ALMT12, a malate-releasing transporter expressing in the plasma membrane of guard cells (Meyer *et al.*, 2010; Sasaki *et al.*, 2010), impaired ABA- and CO_2-induced stomatal closure (Meyer *et al.*, 2010; Sasaki *et al.*, 2010). In addition, exogenous malate at higher than 5 mM induces stomatal closure in a concentration-dependent manner (Hedrich *et al.*, 1994; M. Lee *et al.*, 2008; Araújo *et al.*, 2011) and activates slow-type (S-type) anion channels and rapid-type (R-type) anion channels (Hedrich & Marten, 1993; Raschke, 2003; Konrad & Hedrich, 2008; Wang & Blatt, 2011). Both S-type anion channels and R-type anion channels mediate efflux of anions such as Cl^-, which results in stomatal closure (Keller

et al., 1989; Schroeder & Hagiwara, 1989; Linder & Raschke, 1992; Schroeder & Keller, 1992) whereas pharmacological results suggested that S-type anion channels rather than R-type anion channels contribute to the malate-induced stomatal closure (Schroeder *et al.*, 1993).

In *A. thaliana* guard cells, SLOW ANION CHANNEL-ASSOCIATED1 (SLAC1) and SLAC1 HOMOLOG3 (SLAH3) represent the plasma membrane S-type anion channels (Negi *et al.*, 2008; Vahisalu *et al.*, 2008; Geiger *et al.*, 2011). The mechanism of activation of SLAC1 and SLAH3 in ABA signaling has been well-studied and several protein kinases that phosphorylate and activate SLAC1 and SLAH3, *e.g.* SUCROSE NON-FERMENTING1-RELATED PROTEIN KINASEs (SnRKs) and cytosolic calcium sensor kinase CALCIUM-DEPENDENT PROTEIN KINASEs (CPKs), have been identified (Mustilli *et al.*, 2002; Mori *et al.*, 2006; Geiger *et al.*, 2009; S. C. Lee *et al.*, 2009; Geiger *et al.*, 2011; Brandt *et al.*, 2012; Maierhofer *et al.*, 2014; Brandt *et al.*, 2015). In addition, ABA causes elevation of cytosolic Ca^{2+} concentration ($[Ca^{2+}]_{cyt}$), stimulating Ca^{2+} signaling that activates S-type anion channels (Schroeder & Hagiwara, 1989; Hedrich *et al.*, 1990; Allen *et al.*, 1999; Vahisalu *et al.*, 2008; Siegel *et al.*, 2009; Brandt *et al.*, 2015; Huang *et al.*, 2019). However, the molecular mechanism of malate-induced stomatal closure including regulation of S-type anion channels by malate remains to be clarified.

In this study, I demonstrate that extracellular malate induces stomatal closure by directly activating SLAC1 S-type anion channel in Arabidopsis guard cells.

2.3. Materials and Methods

2.3.1. Plants and growth conditions

All lines of *Arabidopsis thaliana* plants are in the Columbia-0 ecotype. These plants were grown on soil mixture of 1:1 = soil:vermiculite (v/v). The temperature and relative humidity in a growth chamber were 21℃ and 70%, respectively. The photoperiod was 16-h-light/8-h-dark with a photon flux density of 100-μmol m^{-2} s^{-1}. Plants were watered and sprayed twice a week. Rosette leaves from three- to five-week-old plants were used in all experiments.

2.3.2. Measurement of stomatal aperture

Stomatal apertures were measured as described previously (Munemasa *et al*., 2019). Randomly selected rosette leaves were detached and incubated in stomatal assay solution (5 mM KCl, 50 μM $CaCl_2$, and 10 mM MES) for 2 h in the light. The leaves were then transferred to stomatal assay solution supplemented with indicated concentration of L-malic acid for 2 h. All buffers were adjusted to pH 5.6 with Tris. The leaves were shredded in a warner blender and the epidermal tissues were collected with a nylon mesh. The collected epidermis was placed on a glass slide and photographed under an optical microscope (CKX41-31PHP; Olympus) with YCU-300F software (YASHIMA OPTICAL). Twenty stomatal apertures were analyzed for individual experiment with ImageJ software (NIH). The dose-response curve was fitted by the logistic function.

2.3.3. Patch clamp

The whole-cell patch-clamp recording was performed as previously described (Brandt et al., 2015). Randomly selected rosette leaves were shredded in a warner blender, and the epidermal tissues were collected with a nylon mesh. The epidermal tissues incubated in a digestion solution containing 1.0% (w/v) Cellulase R10 (Yakult Pharmaceutical

Industry Co., Tokyo, Japan), 0.5% (w/v) Macerozyme R10 (Yakult Pharmaceutical Industry Co.), 0.5% (w/v) bovine serum albumin, 0.1% (w/v) kanamycin, 10 mM ascorbic acid, 0.1 mM KCl, 0.1 mM $CaCl_2$ and 500 mM D-mannitol (pH 5.5 with KOH) for 14–16 h at 22℃ on a reciprocal shaker at 40 rpm. Guard-cell protoplasts were collected by filtering through a nylon mesh and were then washed with washing solution containing 0.1 mM KCl, 0.1 mM $CaCl_2$, and 500 mM D-sorbitol (pH 5.6 with Tris) by centrifugation for 10 min at 200×*g*. The protoplasts were suspended in the washing solution supplemented with or without 10 mM L-malic acid (pH 5.6 with Tris) and were incubated for 30 min before patch-clamp experiments. The pipette solution contained 150 mM $CsCl_2$, 2 mM $MgCl_2$, 6.7 mM EGTA, 5.86 mM $CaCl_2$, 5 mM Mg-ATP and 10 mM HEPES/Tris (pH 7.1). The bath solution contained 1 mM $CsCl_2$, 2 mM $MgCl_2$ and 1 mM $CaCl_2$, ± 10 mM L-malic acid, and was buffered with 10 mM MES/Tris to adjust pH 5.6. The pipette and bath solutions were adjusted with D-sorbitol to an osmolality of 500 and 485 mOsmol•kg^{-1}, respectively. Steady-state currents were recorded starting from a holding potential of +60 mV and ranging from +65 to −85 mV in 30 mV decrements. The whole-cell currents were recorded using a CEZ-2200 patch-clamp amplifier (NIHON KOHDEN, Tokyo, Japan) and pCLAMP 8.1 software (Molecular Devices, Inc., CA, USA).

2.3.4. Cloning and cRNA synthesis

All constructs were cloned into the oocyte expression vector pNB1u by USER cloning strategy (Nour-Eldin *et al.*, 2006) and In-Fusion® Cloning system (Clontech). The site-directed mutants were generated by KOD -Plus- Mutagenesis Kit (TOYOBO) and In-Fusion® Cloning system (Clontech) according to the manufacturer's instructions. cDNA from *Arabidopsis thaliana* was used for cloning, and all constructs were verified by sequencing. cRNA was prepared with an mMESSAGE mMACHINE^{TM} T7 Transcription Kit (Ambion). Molecular graphics and analyses of SLAC1 were performed with the

PyMOL Molecular Graphics System, Version 2.4.4 Schrödinger, LLC.

2.3.5. Two-electrode voltage-clamp

Xenopus laevis oocytes were injected with 50 nl of water or cRNA (each 10 ng) and incubated in ND96 buffer at 18℃ for a few days before voltage-clamp recordings (Wang *et al.*, 2017). To enhance the interaction of SLAC1 with SnRK2E OPEN STOMATA1 (OST1), I used GFP-fused constructions, SLAC1::sfGFP^{CT} and OST1::sfGFP^{NT}, based on the previous paper (Geiger *et al.*, 2009; Fujii & Kodama, 2015) or the plasma membrane marker-fused construction (Batistič et al., 2008), PM-OST1. The bath solution contained 1 mM Mg-gluconate$_2$, 1 mM Ca-gluconate$_2$ and 1 mM $LaCl_3$, ± 10 mM L-malic acid or L-glutamic acid and was buffered with 10 mM MES/Tris to adjust pH 5.6 or indicated pH. Osmolality was adjusted to 220 mM using D-sorbitol. For a concentration analysis, the bath solution contained the indicated concentration of L-malic acid, was buffered with 10 mM MES/Tris to adjust pH 5.6, and the dose-response curve was fitted by the logistic function. For analyses of effects of intracellular reagents, oocytes were injected 10 mM malate as final concentration or equivalent volume of water and oocytes were recorded consistently 10 min after injections (Wang *et al.*, 2018). Steady-state currents were recorded starting from a holding potential of 0 mV and ranging from +40 or +60 to −160 mV in 20 mV decrements (Geiger *et al.*, 2009). Voltage-clamp recordings for oocytes were performed using an Axoclamp 900A amplilier (Molecular Devices), data were acquired using a Digidata 1440A (Molecular Devices) and analyzed using pCLAMP 10.7 software (Molecular Devices).

2.3.6. Statistical Analysis

For data analysis, Student's *t* test, Welch's *t* test, and ANOVA with Dunnett's test or Tukey's test were used to assess significant differences between datasets. A *P*-value

<0.05 was considered as a significant difference.

2.4. Results

2.4.1. SLAC1 S-type anion channel is essential for malate-induced stomatal closure

The stomatal aperture measurements were carried out with intact leaves. Exogenous malate reduced stomatal aperture at higher than 5 mM and a significant difference was observed at 10 mM (Fig. 2.1a). A half maximal effective concentration (EC_{50}) was 4.3 mM (Fig. 2.1b). In all subsequent experiments, I investigated effects of 10 mM malate.

The malate-induced stomatal closure was disrupted in the *slac1-1* and *slac1-3* mutants but not in the *slah3* mutant (Fig. 2.1c). Complementation of the *slac1* mutants with *SLAC1* recovered the stomatal response to malate (Fig. 2.1c). In contrast to the *slac1* mutations, the mutation of a guard-cell R-type anion channel-encoding gene *QUICK-ACTIVATING ANION CHANNEL1 (QUAC1)* (also known as *ALMT12*) (Meyer *et al.*, 2010; Sasaki *et al.*, 2010) did not impair the malate-induced stomatal closure (Fig. 2.1c). These results suggest that SLAC1 but not either SLAH3 or ALMT12/QUAC1 is involved in the malate-induced stomatal closure. Moreover, the malate-induced stomatal closure was not observed in the *slac1-1* mutants expressing an SLAC1 mutant with S59 and S120 phospho-sites substituted, SLAC1 S59A/S120A (Fig. 2.1c), suggesting that phosphorylation of SLAC1 is required for the malate-induced stomatal closure.

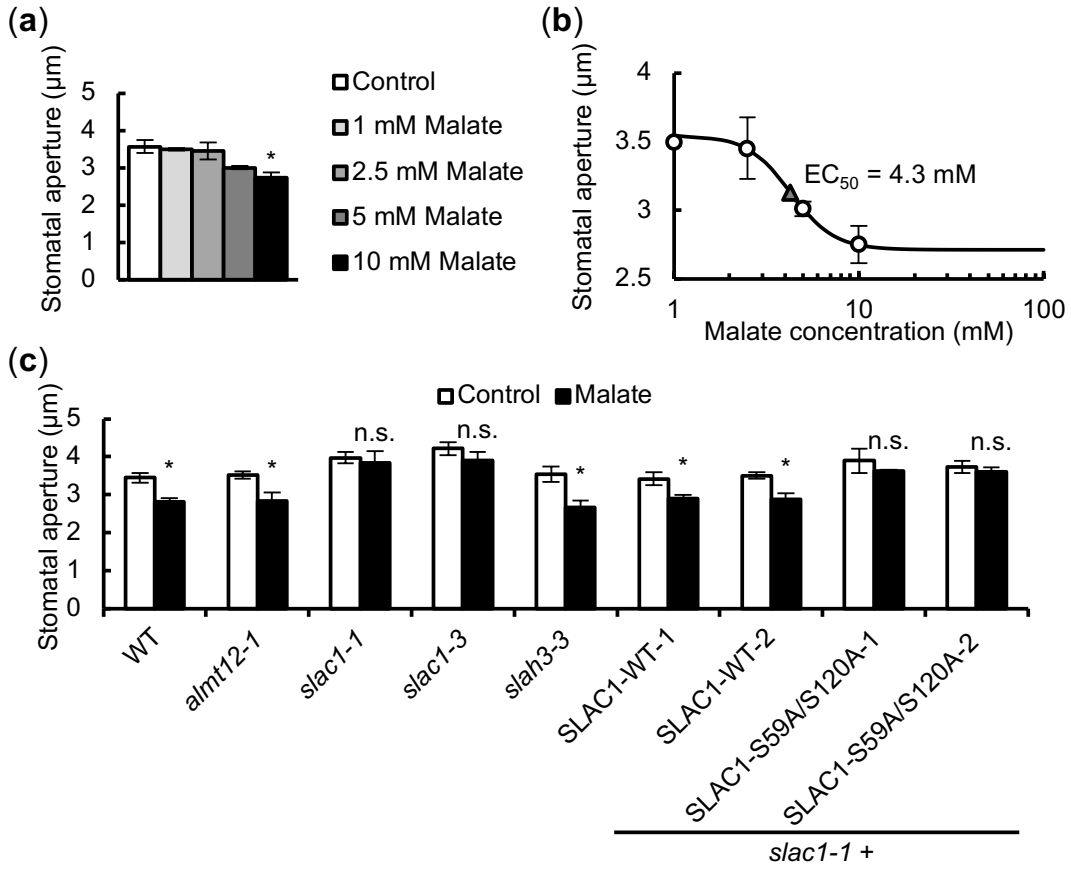

Fig 2.1. SLAC1 is essential for malate-induced stomatal closure in *Arabidopsis thaliana*.

(a) Dose effect of malate on stomatal aperture in wild-type (WT) plants. (b) The dose-response curve was plotted based on (a) and a half maximal effective concentration (EC_{50}; triangle) was 4.3 mM. (c) Malate-induced stomatal closure in *almt12*, *slac1*, and *slah3* deficient mutants and *SLAC1* complemented plants. Averages of stomatal apertures from at least three independent experiments (≥60 total stomata per bar) are shown. Data are mean ± SE. Statistical differences were determined by ANOVA with Dunnett's test (a) and Student's *t* test (c), $*P < 0.05$; n.s., no significant difference.

2.4.2. Malate activates S-type anion channels in Arabidopsis guard cells

I performed whole-cell patch-clamp to examine the effects of malate on S-type anion channels in Arabidopsis guard cells. Extracellular application of malate significantly increased S-type anion currents at −85 mV by 2.0-fold in wild-type plants whereas did not significantly increase or decrease S-type anion currents in the *slac1-1* mutant (Fig. 2.2), suggesting that malate activates SLAC1.

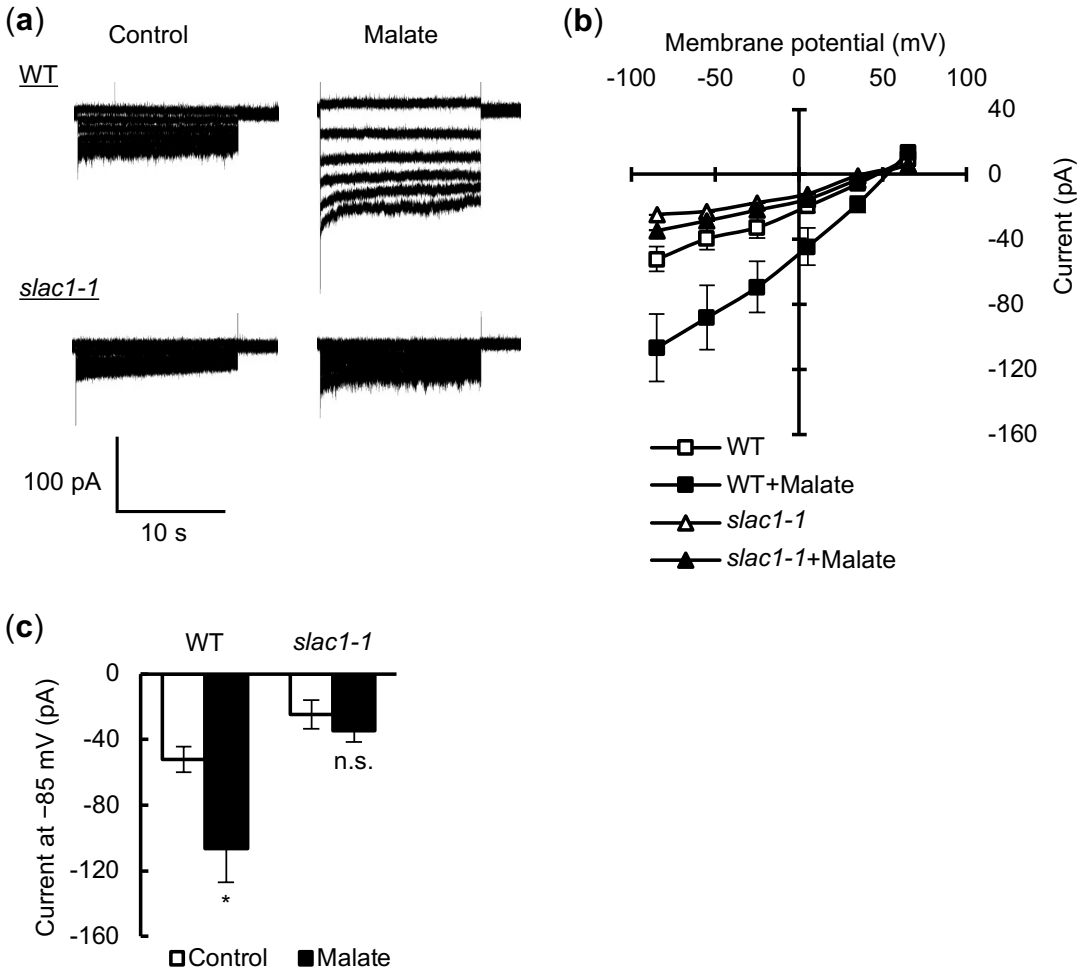

Fig 2.2. The mutation of *SLAC1* impairs extracellular malate activation of S-type anion channel currents in *Arabidopsis thaliana* guard cells.

(a) Representative whole-cell recordings of S-type anion currents in guard-cell protoplasts of wild-type (WT) and *slac1-1* loss-of-function mutant plants in the presence of external malate. The voltage pulse was commanded to clamp the membrane potential from +65 mV to −85 mV in −30 mV steps for 15 seconds with a holding potential of +60 mV. (b) Average steady-state current-voltage curves of whole-cell recordings of S-type anion currents. (c) Average steady-state S-type anion currents at −85 mV. Data were obtained from three to six guard cells for each condition. Data are mean ± SE. Statistical differences were determined by Welch's *t* test, **P* < 0.05; n.s., no significant difference.

2.4.3. Malate activates SLAC1 in the presence of OST1 or CPK6 kinases in Xenopus oocytes

I used two-electrode voltage-clamp to investigate the response of SLAC1 to malate in *Xenopus* oocytes expressing SLAC1 with the kinases OST1 and CPK6, which phosphorylate and activate SLAC1 (Geiger *et al.*, 2009; S. C. Lee *et al.*, 2009; Brandt *et al.*, 2012; Brandt *et al.*, 2015). The negative currents in the oocytes expressing SLAC1 without kinases were not significantly larger than those in the oocytes injected water as a control (Fig. 2.3); the negative currents in the oocytes expressing SLAC1 with OST1 and with CPK6 were significantly larger 2.9-fold and 2.8-fold at −160 mV than those in the oocytes expressing SLAC1, respectively (Fig. 2.3c, 2.4c). The application of malate did not significantly increase the negative currents in the oocytes either injected water or expressing SLAC1. On the other hand, the application of malate significantly increased the SLAC1 currents at −160 mV by 1.6-fold in the oocytes expressing both SLAC1 and OST1 (Fig. 2.3c) and by 1.9-fold in the oocytes expressing both SLAC1 and CPK6 (Fig. 2.4c).

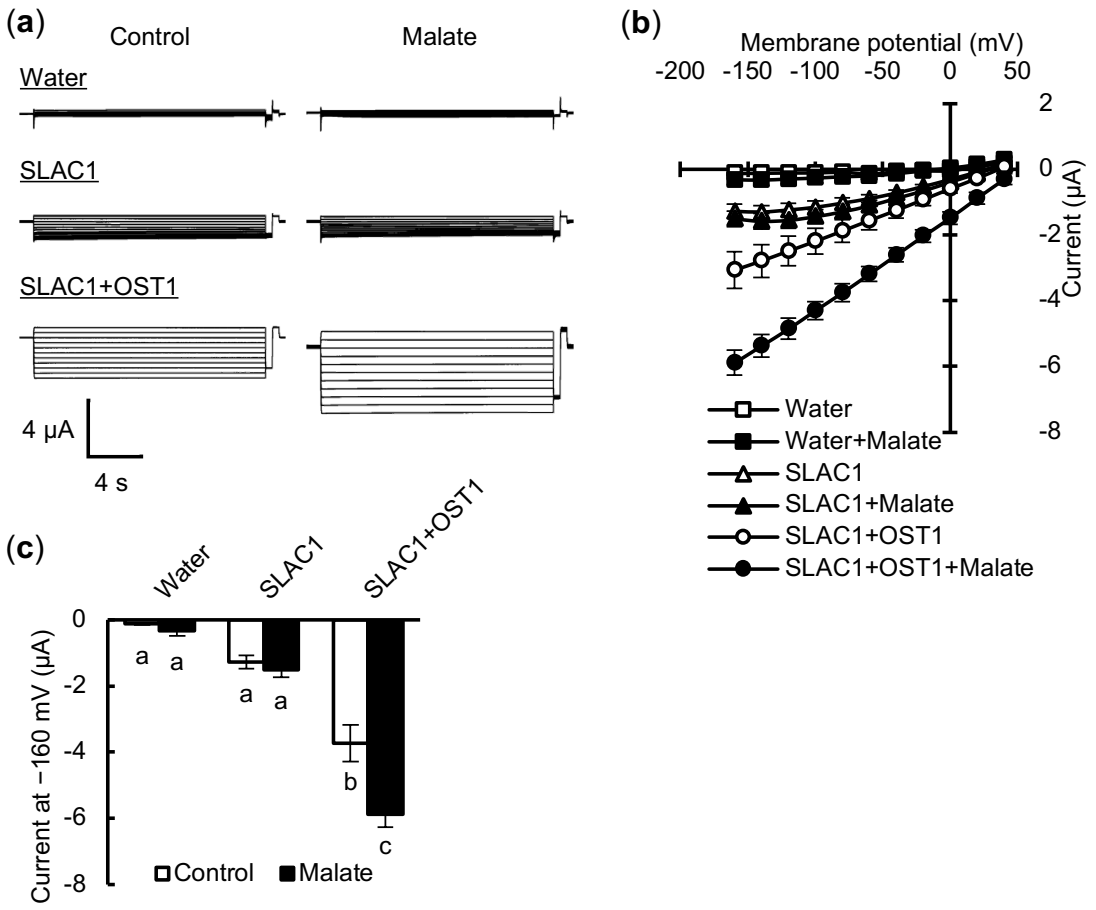

Fig 2.3. Extracellular malate activates SLAC1 in the presence of OST1 kinase in *Xenopus* oocytes.

(a) Representative whole-cell negative current recordings in *Xenopus* oocytes expressing SLAC1 or SLAC1 with OST1 kinase in the presence of external malate. The voltage pulse was commanded to clamp the membrane potential from +40 mV to −160 mV in −20 mV steps for 17 seconds with a holding potential of 0 mV. (b) Average steady-state current-voltage curves of whole-cell negative current recordings. (c) Average steady-state negative currents at −160 mV. Data were obtained from four oocytes per condition. Data are mean ± SE. Different letters indicate statistical significances based on ANOVA with Tukey's test, $P < 0.05$.

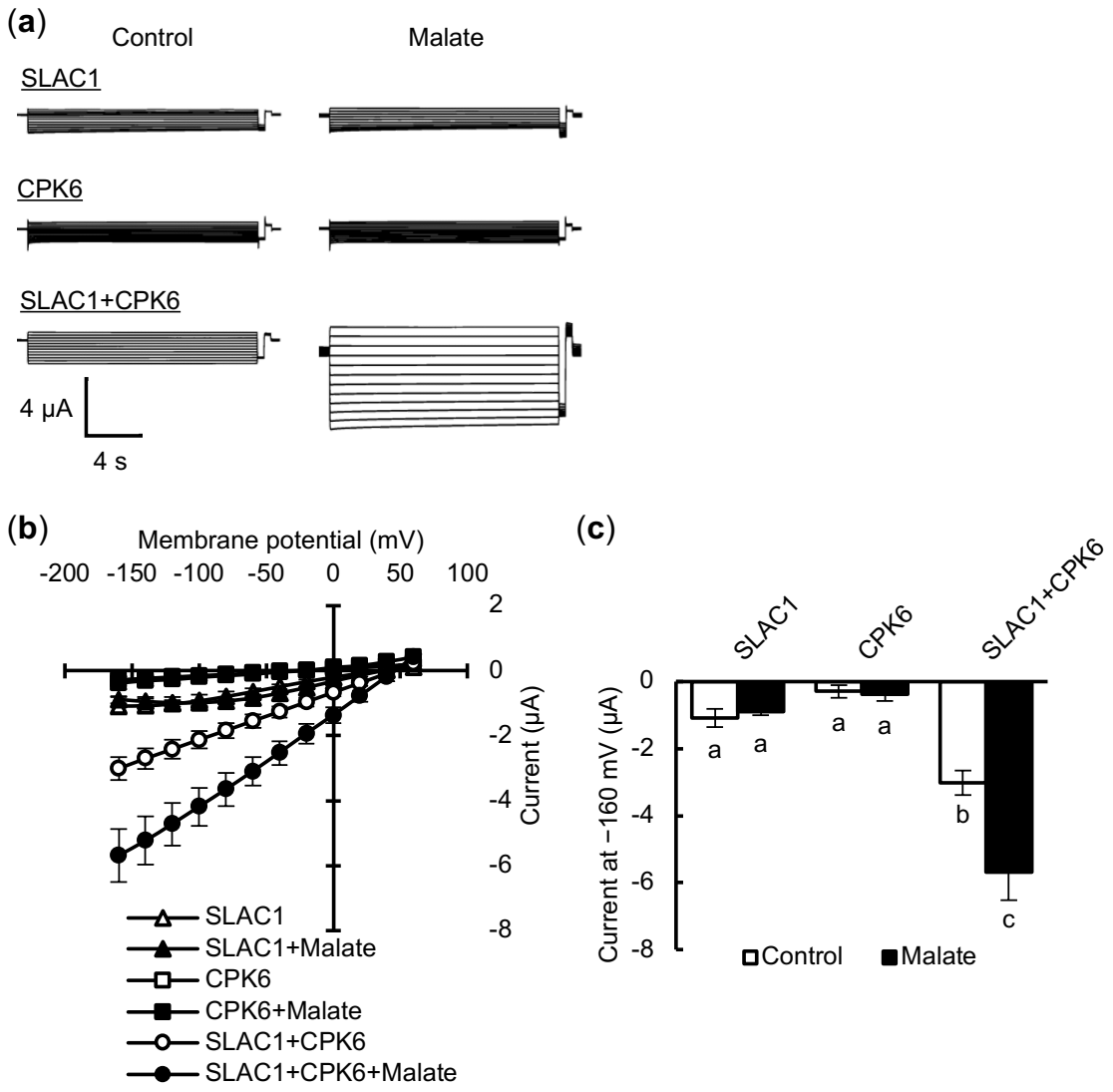

Fig 2.4. Extracellular malate activates SLAC1 in the presence of CPK6 kinase in *Xenopus* oocytes.

(a) Representative whole-cell negative current recordings in *Xenopus* oocytes expressing SLAC1 or SLAC1 with CPK6 kinase in the absence or presence of external malate. The voltage pulse was commanded to clamp the membrane potential from +60 mV to −160 mV in −20 mV steps for 17 seconds with a holding potential of 0 mV. (b) Average steady-state current-voltage curves of whole-cell negative current recordings. (c) Average steady-state negative currents at −160 mV. Data were obtained from five oocytes per condition. Data are mean ± SE. Different letters indicate statistical significances based on ANOVA with Tukey's test, $P < 0.05$.

2.4.4. Malate directly activates constitutively active mutants of SLAC1 without kinases

I expressed two types of constitutively active SLAC1 mutants, an opened gate mutant SLAC1F450A and a phosphorylation-mimetic mutant SLAC1T513D in the oocytes (Chen *et al.*, 2010; Maierhofer *et al.*, 2014). The SLAC1 currents in the oocytes expressing SLAC1F450A or SLAC1T513D were significantly larger than those in the oocytes expressing SLAC1 (Fig. 2.5). The application of malate significantly increased the SLAC1 currents at −160 mV by 1.6-fold in both oocytes expressing SLAC1F450A and oocytes expressing SLAC1T513D (Fig. 2.5c). These results suggest that malate directly activates the phosphorylated SLAC1. In addition, exogenous malate significantly increased the SLAC1 currents in the oocytes expressing SLAC1T513D at higher than 5 mM but not at lower than 5 mM (Fig. 2.6a–c). EC_{50} was 8.2 mM and a slope *S* was 2.3 at −160 mV (Fig. 2.6d), demonstrating that malate is an allosteric activator of SLAC1.

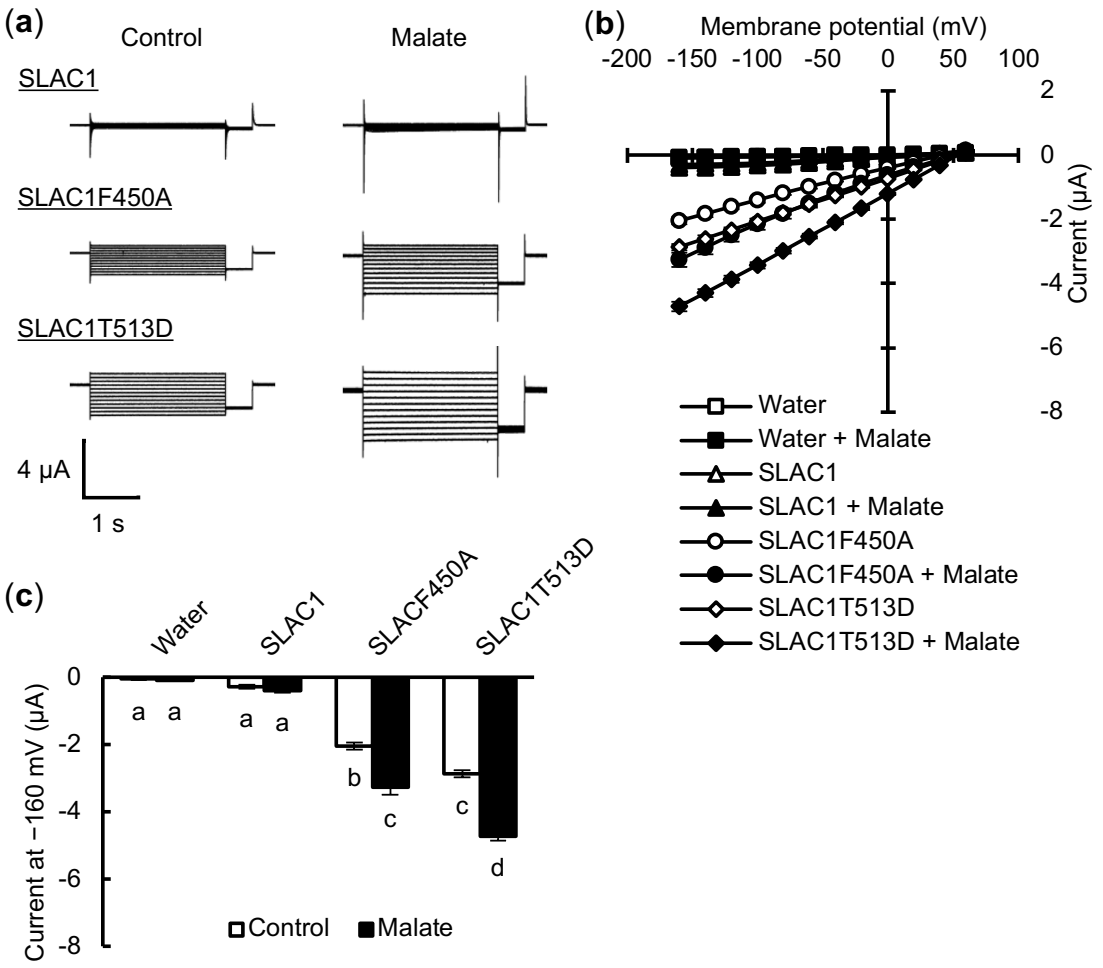

Fig 2.5. Extracellular malate directly activates constitutively active mutants of SLAC1 without kinases in *Xenopus* oocytes.

(a) Representative whole-cell negative current recordings in *Xenopus* oocytes expressing SLAC1 or constitutively active mutants of SLAC1 in the presence of external malate. The voltage pulse was commanded to clamp the membrane potential from +60 mV to −160 mV in −20 mV steps for 2.5 seconds with a holding potential of 0 mV. (b) Average steady-state current-voltage curves of whole-cell negative current recordings. (c) Average steady-state negative currents at −160 mV. Data were obtained from six oocytes per condition. Data are mean ± SE. Different letters indicate statistical significances based on ANOVA with Tukey's test, $P < 0.05$.

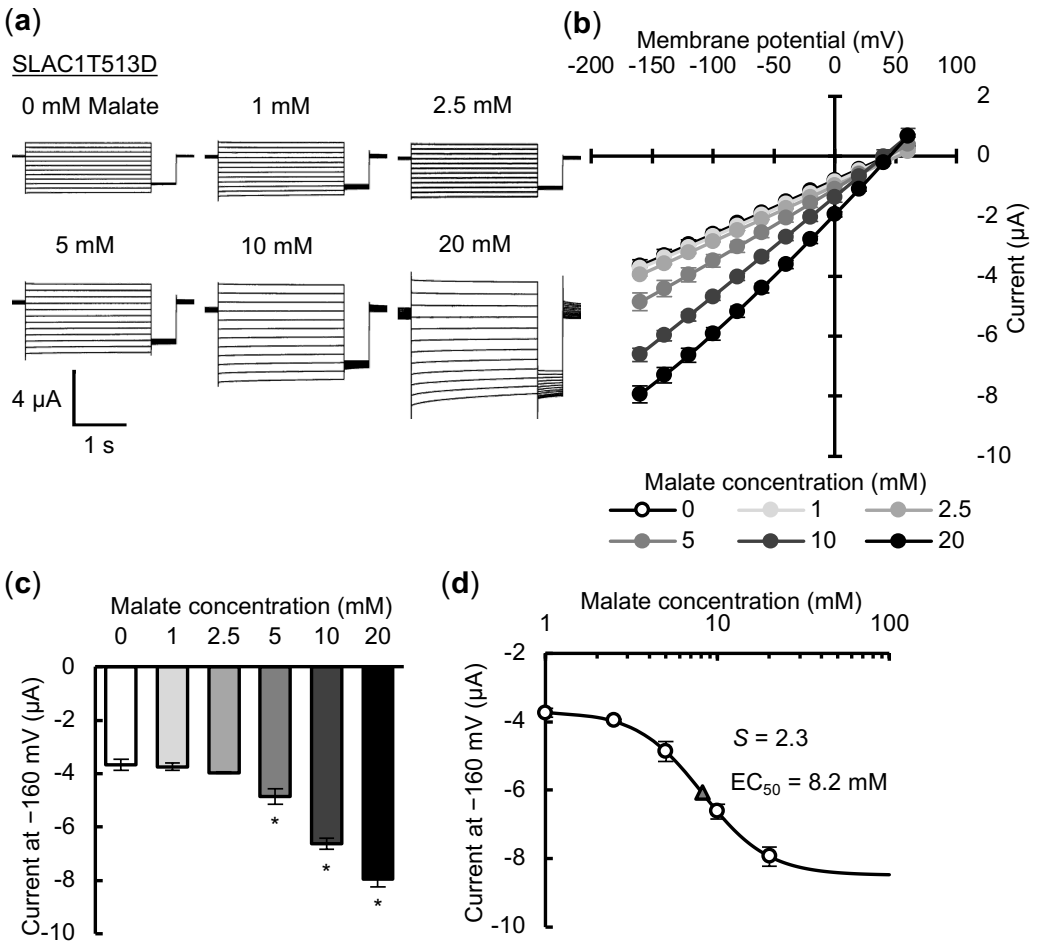

Fig 2.6. Extracellular malate activates the constitutively active mutant of SLAC1 in a concentration-dependent manner in *Xenopus* oocytes.

(a) Representative whole-cell negative current recordings in *Xenopus* oocytes expressing SLAC1T513D in the presence of the indicated concentrations of external malate. The voltage pulse was commanded to clamp the membrane potential from +60 mV to −160 mV in −20 mV steps for 2.5 seconds with a holding potential of 0 mV. (b) Average steady-state current-voltage curves of whole-cell negative current recordings. (c) Average steady-state negative currents at −160 mV. (d) The dose-response curve was plotted based on (c). A half maximal effective concentration (EC_{50}; triangle) was 8.2 mM and a slope *S* was 2.3. Data were obtained from six oocytes per condition. Data are mean ± SE. Statistical differences were determined by ANOVA with Dunnett's test, $^*P < 0.05$.

2.4.5. Intracellular malate does not act on SLAC1

I injected malate into the oocytes expressing SLAC1 and SLAC1T513D. Note that the intracellular malate is estimated at 10 mM based on the diameter of oocytes. The injection of malate did not increase or decrease the SLAC1 currents (Fig. 2.7), which is consistent with the recent result that intracellular malate at approximately 10 mM did not affect SLAC1 activity in the oocytes expressing OST1 (Wang *et al.*, 2018). This result suggests that intracellular malate does not modulate SLAC1 activities.

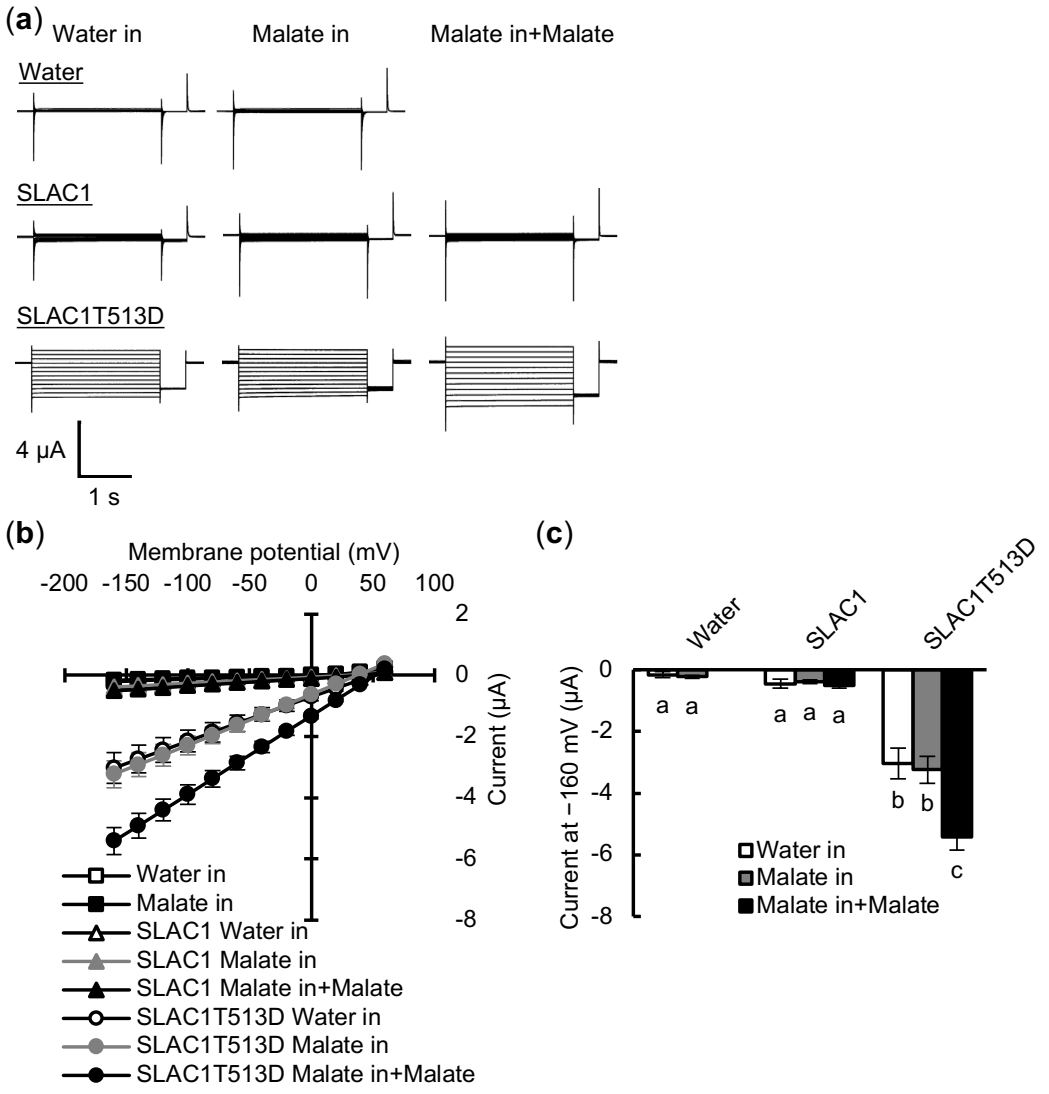

Fig 2.7. Intracellular malate at 10 mM does not modulate the activity of SLAC1 in *Xenopus* oocytes.

(a) Representative whole-cell negative current recordings in *Xenopus* oocytes expressing SLAC1 or the constitutively active mutant of SLAC1 in the presence of internal malate. The voltage pulse was commanded to clamp the membrane potential from +60 mV to −160 mV in −20 mV steps for 2.5 seconds with a holding potential of 0 mV. (b) Average steady-state current-voltage curves of whole-cell negative current recordings. (c) Average steady-state negative currents at −160 mV. Data were obtained from four oocytes per condition. Data are mean ± SE. Different letters indicate statistical significances based on ANOVA with Tukey's test, $P < 0.05$.

2.4.6. Malate activates constitutively active mutants of SLAC1 in a pH-dependent manner

The application of malate at pH 5.6 significantly increased the SLAC1 currents at −160 mV in oocytes expressing SLAC1T513D (Fig. 2.8). The application of malate at pH 3.1 or pH 4.0 did not increase or decrease the SLAC1 currents at −160 mV in oocytes expressing SLAC1T513D (Fig. 2.8). In addition, the application of glutamate at pH 5.6 did not increase or decrease the SLAC1 currents at −160 mV in oocytes expressing SLAC1T513D (Fig. 2.8). These results indicates that the acidic conditions (pH 3.1 and pH 4.0) abolished the malate activation of SLAC1 (Fig. .2.8).

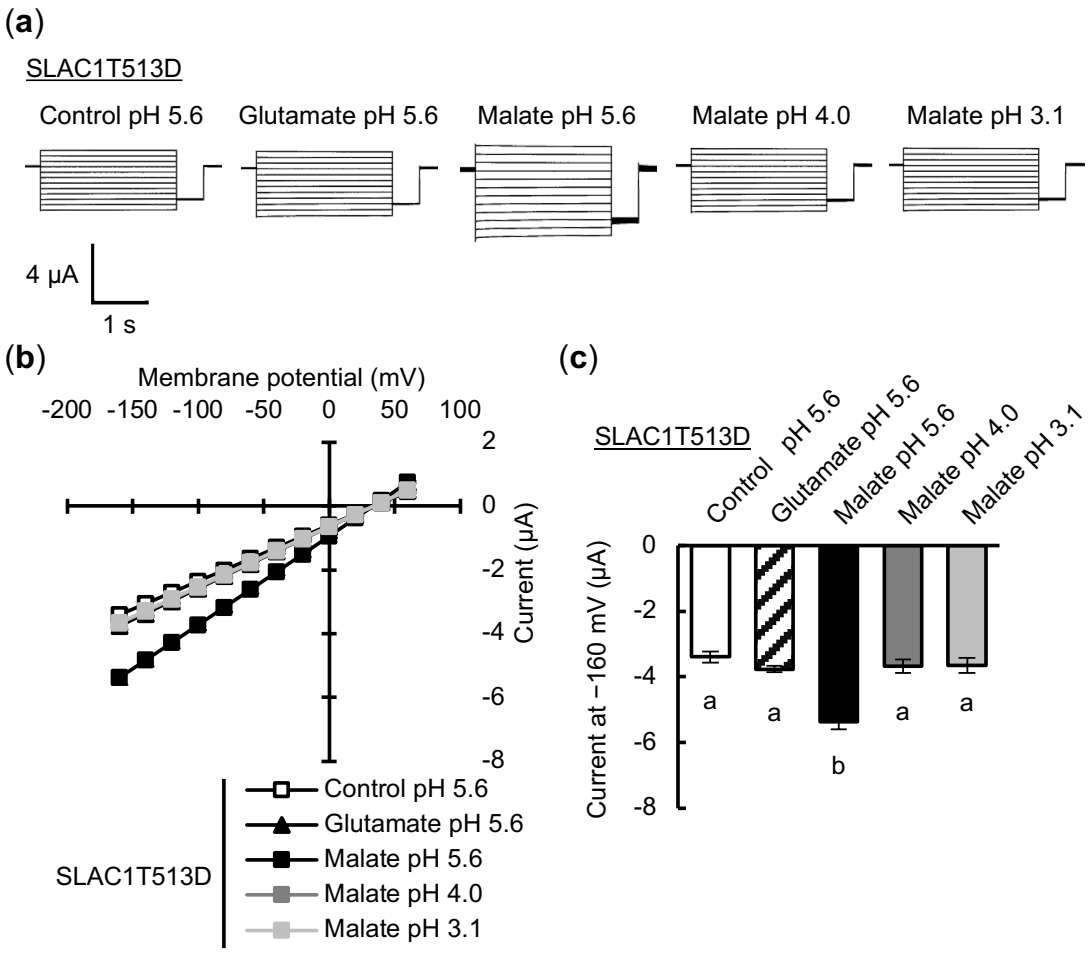

Fig 2.8. The acidic conditions abolish the malate activation of SLAC1 in *Xenopus* oocytes.

(a) Representative whole-cell negative current recordings in *Xenopus* oocytes expressing the constitutively active mutant of SLAC1 in the presence of external malate or glutamate at indicated pH. The voltage pulse was commanded to clamp the membrane potential from +60 mV to −160 mV in −20 mV steps for 2.5 seconds with a holding potential of 0 mV. (b) Average steady-state current-voltage curves of whole-cell negative current recordings. (c) Average steady-state negative currents at −160 mV. Data were obtained from four oocytes per condition. Data are mean ± SE. Different letters indicate statistical significances based on ANOVA with Tukey's test, $P < 0.05$.

2.5. Discussion

I demonstrated that exogenous malate induces stomatal closure and activates S-type anion channels of guard-cell plasma membrane in Arabidopsis wild-type plants, but not in the *slac1* mutants (Fig. 2.1, 2.2). Moreover, I found that exogenous malate directly activates SLAC1 (Fig. 2.5). These results suggest that extracellular malate functions as an SLAC1 potential ligand that regulates stomatal movements in *A. thaliana*. In the kinetic analyses of the malate activation, both EC_{50} for stomatal closure (4.3 mM) and for SLAC1 activation (8.2 mM) were within the physiological concentration considering the leaf apoplastic concentrations of malate from various species (0.2 mM to 10 mM: Welbaum and Meinzer, 1990; Lohaus et al., 1995; Mühling and Sattelmacher, 1995; Gabriel & Kesselmeier, 1999; Hedrich et al., 2001) and *S* of 2.3 was acceptable because SLAC1 forms a symmetrical trimer (Chen *et al.*, 2010; Deng *et al.*, 2021).

The acidic conditions (pH 3.1 and pH 4.0) abolished the malate activation of SLAC1 (Fig. 2.8). Since pKa_1 and pKa_2 of malate are 3.4 and 5.1, respectively, double-deprotonated form of malate dominates at pH 5.6. This result suggests that divalent malate activates SLAC1 and that charged amino residues of SLAC1 are involved in the malate sensing. The activation of SLAC1 by malate is likely to occur along with the apoplastic pH elevation under the physiological condition because the apoplastic pH is increased by the treatment with malate (Hedrich *et al.*, 2001). As for glutamate, divalent glutamate is a major component at pH 5.6 because pKa1 and pKa2 are 2.1 and 4.1, respectively, however, glutamate was not able to activate SLAC1 (Fig. 2.8). This result indicates that glutamate is not a ligand of SLAC1.

The direct activation of SLAC1 by extracellular malate required the phosphorylation of SLAC1 by the protein kinases (Fig. 2.3, 2.4). This result is consistent with this study that the non-phosphorylatable SLAC1 mutants were insensitive to application of malate (Fig. 2.1c). There should be a two-step pathway in which

extracellular malate activates SLAC1. First step is the phosphorylation of SLAC1 as a priming effect. Extracellular malate stimulated stomatal closure signaling and SLAC1 is phosphorylated by protein kinases. Second step is the direct activation of SLAC1. Extracellular malate directly activates SLAC1 pre-phosphorylated through the first step. Through these two distinct mechanisms, extracellular malate efficiently and effectively activates SLAC1.

Mesophyll signals with the molecule size between 100 Da and 1000 Da are produced at high CO_2 condition and induced stomatal closure (Fujita *et al.*, 2013). Since the molecular mass of malate is 134 Da and the concentration of apoplastic malate is increased up to several mM at high [CO_2] (Hedrich *et al.*, 1994), malate is thought to be one of mesophyll signals. Malate exporters Mesophyll cells may perceive increase in [CO_2] and secrete malate through malate exporters such as ALMTs. The secreted malate contributes to activation of SLAC1 in the guard cells, leading to stomatal closure. In this case, malate importers also play important roles. For example, plants lacking a malate importer *ABC TRANSPORTER B family member 14 (ABCB14)* show stronger malate-induced stomatal closure (M. Lee *et al.*, 2008). Malate importers should have the function of retrieving the secreted malate and controlling the stomatal response. This system like a synaptic transmission would allow independent and isolated guard cells without plasmodesmata to communicate with mesophyll cells to response environmental stresses.

CHAPTER3

Malate induces stomatal closure *via* a receptor-like kinase GHR1-, reactive oxygen species- and cytosolic calcium-dependent pathway in *Arabidopsis thaliana*

3.1. Abstract

A primary metabolite malate is secreted from guard cells in response to the phytohormone abscisic acid (ABA) and the secreted malate induces stomatal closure in plants. Here I investigated the molecular mechanism of malate-induced stomatal closure using inhibitors and ABA signaling component mutants of *Arabidopsis thaliana*. Malate-induced stomatal closure was impaired by a protein kinase inhibitor, K252a. The malate-induced stomatal closure was impaired by the disruption of a receptor-like kinase GHR1, which mediates activation of Ca^{2+} channel by reactive oxygen species (ROS) in guard cells. Malate induced ROS production in guard cells while the malate-induced stomatal closure was impaired by a peroxidase inhibitor, salicylhydroxamic acid but not by the disruption of NAD(P)H oxidases RBOHD and RBOHF. The treatment with malate transiently increased cytosolic Ca^{2+} concentration in the wild-type guard cells and the malate-induced stomatal closure was inhibited by the Ca^{2+} channel blockers and the Ca^{2+} chelators. These results demonstrate that the malate signal is mediated by the signaling component GHR1 and second messengers ROS and Ca^{2+} in Arabidopsis guard cells.

3.2. Introduction

Plants adjust stomatal aperture in response to changes in the environment in order to control the amount of water loss and gas exchange. Stomatal pores are formed by a pair of guard cells in the epidermis of leaves and stomatal movements are accompanied by

transports of osmolytes across the plasma membrane of guard cells (Schroeder *et al.*, 2001). A primary metabolite malate represents a major organic osmolyte in guard cells. Malate is secreted from guard cells and mesophyll cells in response to a phytohormone abscisic acid (ABA) or elevated CO_2 (Van Kirk & Raschke, 1978; Kondo & Maruta, 1987; Hedrich *et al.*, 1994). External application of malate induces stomatal closure in a concentration-dependent manner (Hedrich *et al.*, 1994; Esser *et al*., 1997). Furthermore, malate activates slow (S-type) anion channels (Wang & Blatt, 2011). Activation of S-type anion channels cause membrane depolarization, followed by activation of voltage-dependent K^+_{out} channels, decreasing turgor pressure of the guard cell and promoting stomatal closure (Schroeder *et al.*, 2001). However, the mechanism by which malate regulates anion channels remains unclear.

S-type anion channels are activated through phosphorylation by protein kinases. In *Arabidopsis thaliana*, a receptor-like kinase GUARD CELL HYDROGEN PEROXIDE-RESISTANT1 (GHR1), cytosolic calcium ion (Ca^{2+}) sensor kinases CALCIUM-DEPENDENT PROTEIN KINASEs (CPKs) and a Ca^{2+}-independent protein kinase OPEN STOMATA1 (OST1) are identified as main protein kinases which regulate the activity of S-type anion channels (Mori *et al*., 2006; Brandt *et al.*, 2015; Hua *et al*., 2012). Furthermore, the activity of these protein kinases is regulated by PROTEIN PHOSPHATASE 2Cs (PP2Cs), such as ABA INSENSITIVE1 (ABI1) and ABI2, and ABA receptors, PYRABACTIN RESISTANCE1 (PYR1)/PYR1-LIKE (PYL)/REGULATORY COMPONENT OF ABA RECEPTOR (RCAR), in response to ABA (Geiger *et al*., 2009; Lee *et al*., 2009; Geiger *et al*., 2010; Hua *et al*., 2012).

Reactive oxygen species (ROS) and cytosolic Ca^{2+} function as second messengers in guard cells and induce stomatal closure (Pei *et al*., 2000). ROS activate plasma membrane Ca^{2+} channels. Activated Ca^{2+} channels cause Ca^{2+} influx and elevation of cytosolic Ca^{2+} concentration ($[Ca^{2+}]_{cyt}$), which activates CPKs (Pei *et al*.,

2000; Mori *et al*., 2006). ROS are produced mainly by apoplastic peroxidases in salicylic acid signaling (Mori *et al*., 2001; Khokon *et al*., 2011) and by NAD(P)H oxidases RESPIRATORY BURST OXIDASE HOMOLOGs (RBOHs) in ABA signaling (Kwak *et al*., 2003). Salicylic acid-induced stomatal closure is impaired by a peroxidase inhibitor salicylhydroxamic acid (SHAM)-sensitive (Mori *et al*., 2001; Khokon *et al*., 2011) and ABA-induced stomatal closure is impaired by an NAD(P)H oxidase inhibitor diphenyleneiodonium chloride (DPI) (Pei *et al*., 2000).

In order to clarify the molecular mechanism of malate-induced stomatal closure, I investigated effects of malate on stomatal response using inhibitors and ABA signaling component mutants of *Arabidopsis thaliana*.

3.3. Materials and methods

3.3.1. Plants and growth conditions

All lines of *Arabidopsis thaliana* plants are in the Columbia-0 ecotype. The mutants used in this study were *pyr1 pyl1 pyl2 pyl4 pyl5 pyl8* (CS72392), *abi1-1C* (a dominant negative mutant), *abi2-1C* (a dominant negative mutant), *ost1-3* (SALK_008068), *cpk3-1 cpk6-2* (a mutant crossed SALK_107620 and SALK_033392), *ghr1-6* (SALK_031493), *ht1-9* (a kinase-dead mutant) and *rbohD rbohF* (*atrbohD atrbohF*). Plants were grown on soil mixture of 1:1 = soil:vermiculite (v/v) in a growth chamber at 21℃ and 70% relative humidity under 16-h-light/8-h-dark photoperiod with a photon flux density of 100 μmol m^{-2} s^{-1}. Plants were watered and sprayed twice a week. Three- to five-week-old plants were used in all experiments.

3.3.2. Measurement of stomatal aperture

Stomatal apertures were measured as described previously (Munemasa *et al*., 2019). Randomly selected rosette leaves were detached and incubated in stomatal assay solution (5 mM KCl, 50 μM $CaCl_2$, and 10 mM MES) for 2 h in the light. The leaves were then transferred to stomatal assay solution supplemented with 10 mM L-malic acid, 10 mM L-glutamic acid or 100 μM L-methionine for 2 h. All buffers were adjusted to pH 5.6 with Tris. For treatment with K252a, SHAM, DPI, and W7, after 1.5-h incubation in stomatal assay solution, the leaves were treated with each inhibitor for 30 min in the absence of malate and then for 2 h in the presence of malate. For 1,2-bis(2-aminophenoxy)ethane-*N*,*N*,*N'*,*N'*-tetraacetic acid (BAPTA), $LaCl_3$, verapamil, and niflumic acid treatment, after 2-h incubation in the absence of malate, the leaves were treated with each reagents in the presence of malate. For BAPTA-acetoxymethyl ester (BAPTA-AM) treatment, after 110-min incubation in the absence of malate, the leaves were treated with BAPTA-AM for 10 min in stomatal assay solution excluding $CaCl_2$

added 25 μM BAPTA-AM, 0.3 mM eserine and 0.025% Pluronic F-127, and then for 1 h in stomatal assay buffer excluding $CaCl_2$ containing 10 mM L-malic acid added 25 μM BAPTA-AM and 0.025% Pluronic F-127 as described previously (Siegel *et al.*, 2009) with a few modifications. The leaves were shredded in a warner blender and the epidermal tissues were collected with a nylon mesh. The collected epidermis was placed on a glass slide and photographed under an optical microscope (CKX41-31PHP; Olympus) with YCU-300F software (YASHIMA OPTICAL). Twenty or 60 stomatal apertures were analyzed for individual experiment with ImageJ software (NIH).

3.3.3. Measurement of ROS accumulation

ROS accumulation in guard cells was evaluated using the fluorescent dye 2',7'-dihydrodichlorofluorescein diacetate (H_2DCF-DA) as described previously (Munemasa *et al.*, 2019). Randomly selected rosette leaves were detached and shredded in a warner blender. The epidermal tissues were collected using a nylon mesh and incubated in stomatal assay solution in the light for 3 h. Fifty micromolar H_2DCF-DA was added to stomatal assay solution and the epidermal tissues were incubated in the dark for 30 min. After the dye loading, the epidermal tissues were collected using a nylon mesh and gently rinsed with stomatal assay solution. The tissues were resuspended in stomatal assay solution and then incubated with or without 10 mM L-malic acid or 50 μM ABA. After the 30-min incubation, fluorescent signals were captured using a fluorescence microscope (Biozero BZ-8000, Keyence, Osaka, Japan) and analyzed using ImageJ 1.42q software (NIH, USA).

3.3.4. $[Ca^{2+}]_{cyt}$ imaging

Wild-type plants expressing YC3.6 were used for the measurement of $[Ca^{2+}]_{cyt}$ in guard cells as described previously (Ye *et al.*, 2020). The abaxial side of an excised rosette leaf

was gently attached to a glass slide with a medical adhesive (stock no. 7730; Hollister) and then mesophyll tissues were cut off with a razor blade to keep the abaxial epidermis intact on the slide. The remaining abaxial epidermis was immersed in stomatal assay solution in the light for 2h at 22℃ to induce stomatal opening. Guard cells were treated with 10 mM L-malic acid and L-glutamic acid by perfusion of stomatal assay solution containing 10 mM L-malic acid or L-glutamic acid at 5 min after monitoring and all guard cells were treated with $CaCl_2$ by perfusion of stomatal assay solution added 10 mM $CaCl_2$ at 20 min after the measurement. Fluorescence intensity from the cyan fluorescent protein and yellow fluorescent protein in guard cells were imaged and analyzed using the W-View system and AQUA COSMOS software (Hamamatsu Photonics).

3.3.5. Statistical analysis

The significance of differences between the mean values of data sets was assessed by Student's *t*-test and χ^2 test. Differences at the level of $P < 0.05$ were considered to be significant.

3.4. Results

3.4.1. Malate-induced stomatal closure in the presence of protein kinase inhibitors or in mutants of protein kinases

The exogenous application of malate significantly induced stomatal closure in the abaxial side of Arabidopsis rosette leaves (Fig 3.1a). Malate did not significantly reduce the stomatal aperture in the presence of a protein kinase inhibitor K252a (Fig 3.1a). Malate significantly reduced stomatal aperture in the wild-type plants but not in the *ghr1-6* mutant (Fig 3.1b). Malate significantly reduced stomatal aperture in the *ost1-3* and *cpk3-1 cpk6-2* mutants and the mutant of a mitogen-activated protein kinase kinase kinase (MAPKKK) HIGH LEAF TEMPERATURE1 (HT1) (Fig 3.1b).

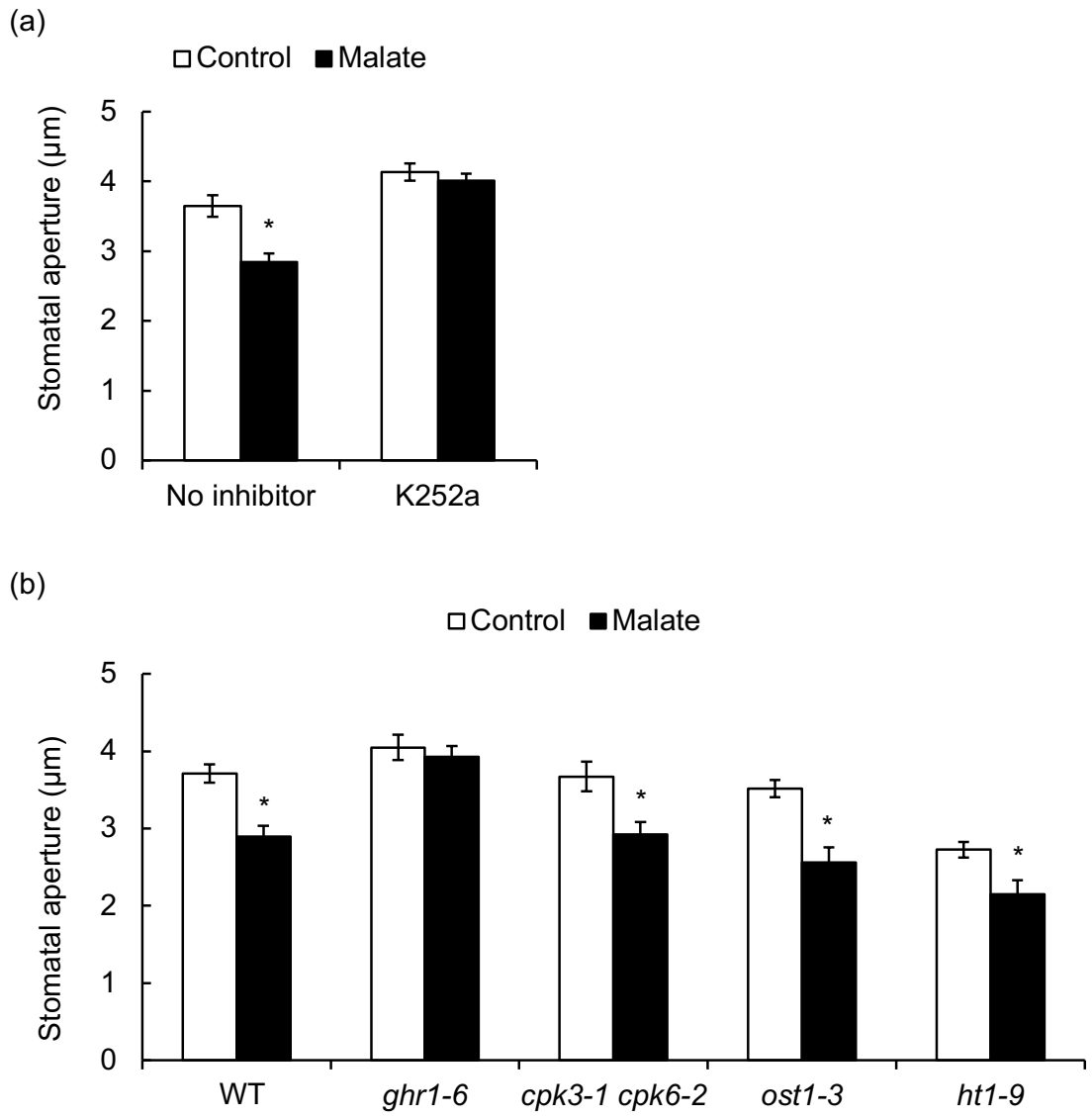

Fig 3.1. Malate-induced stomatal closure in the presence of protein kinase inhibitor or in mutants of protein kinases.

(a) Effects of 10 mM malate on stomatal aperture in the presence of 1 μM K252a in wild-type plants. (b) Effects of 10 mM malate on stomatal aperture in the *ghr1-6*, *cpk3-1 cpk6-2*, *ost1-3* and *ht1-9* mutants. Averages of stomatal apertures from at least three independent experiments (≥60 total stomata per bar) are shown. Data are mean ± SE. Asterisk denotes a significant difference vs. corresponding control ($P < 0.05$).

3.4.2. Malate-induced stomatal closure in mutants deficient in ABA signaling components

The exogenous application of malate significantly reduced stomatal aperture in the *pyr1 pyl1 pyl2 pyl4 pyl5 pyl8*, *abi1-1C*, and *abi2-1C* mutants as well as wild-type plants (Fig 3.2).

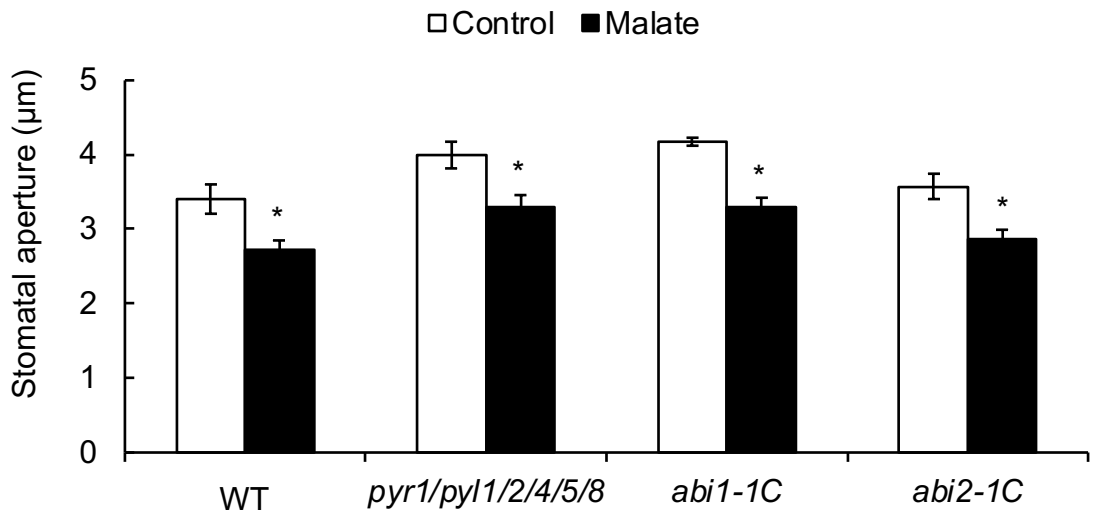

Fig 3.2. Malate-induced stomatal closure in mutants of ABA signaling components. Effects of 10 mM malate on stomatal aperture in the *pyr1 pyl1 pyl2 pyl4 pyl5 pyl8*, *abi1-1C* and *abi2-1C* mutants. Averages of stomatal apertures from at least three independent experiments (≥60 total stomata per bar) are shown. Data are mean ± SE. Asterisk denotes a significant difference vs. corresponding control ($P < 0.05$).

3.4.3. Malate-induced ROS production in guard cells

Malate as well as ABA induced ROS accumulation in guard cells (Fig 3.3a). The malate-induced stomatal closure was impaired by a peroxidase inhibitor SHAM but not by an NAD(P)H oxidase inhibitor DPI (Fig 3.3b). In addition, the malate-induced stomatal closure was not impaired in the *rbohD rbohF* double mutant (Fig 3.3c).

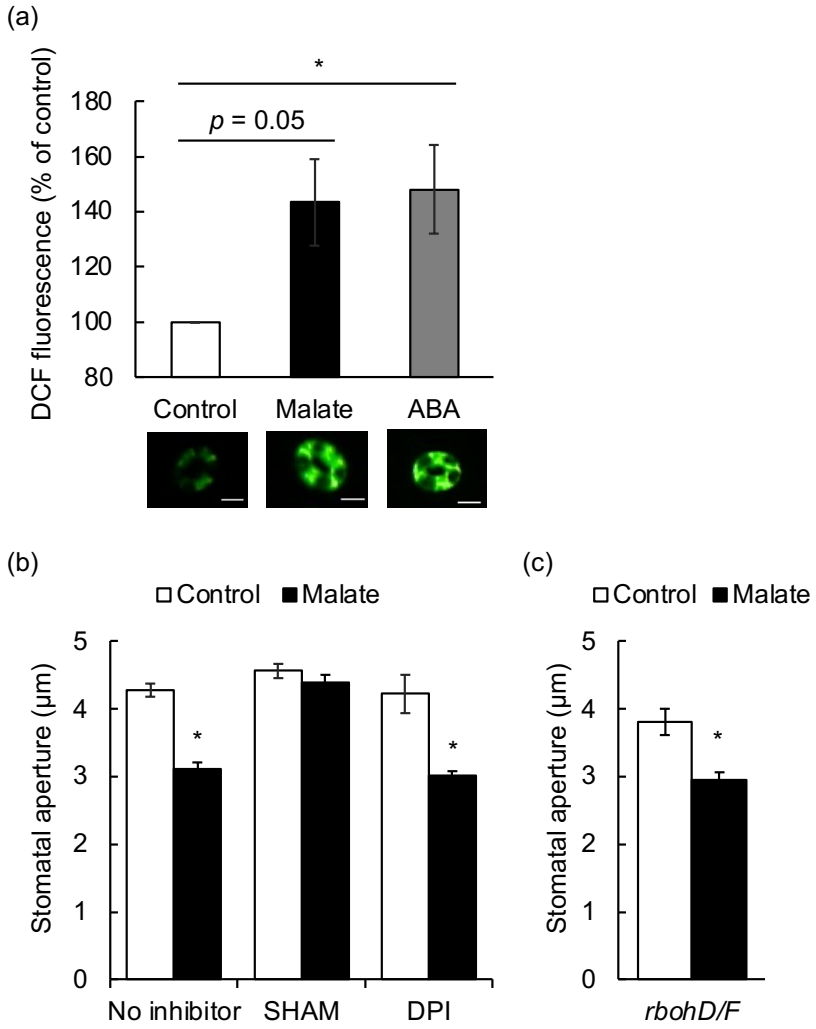

Fig 3.3. Malate-induced ROS production in guard cells.

(a) Effects of 10 mM malate or 50 μM ABA on ROS production in guard cells of wild-type plants. The ROS-sensitive dye, 2',7'-dichlorodihydrofluorescein diacetate (H_2DCF-DA) was used for ROS detection in guard cells. Scale bar = 10 μm. Fluorescence intensity was normalized to the control values. Averages from three independent experiments (>380 guard cells per bar in total) are shown. (b) Effects of 10 mM malate on stomatal aperture in the presence of 20 μM DPI or 2 mM SHAM in wild-type plants. (c) Effects of 10 mM malate on stomatal aperture in the *rbohD rbohF* mutant. Averages of stomatal apertures from at least three independent experiments (≥60 total stomata per bar) are shown. Data are mean ± SE. Asterisk denotes a significant difference vs. corresponding control ($P < 0.05$).

3.4.4. Malate-induced stomatal closure in the presence of Ca^{2+} channel blockers.

The malate-induced stomatal closure was impaired by an extracellular Ca^{2+} chelator BAPTA and a non-selective Ca^{2+} channel blocker La^{3+} (Fig. 3.4a). The malate-induced stomatal closure was inhibited by voltage-dependent Ca^{2+} channel blockers verapamil and niflumic acid (Fig 3.4b). In addition, the malate-induced stomatal closure was not impaired by a calmodulin (CaM) antagonist W7 (Fig 3.4b).

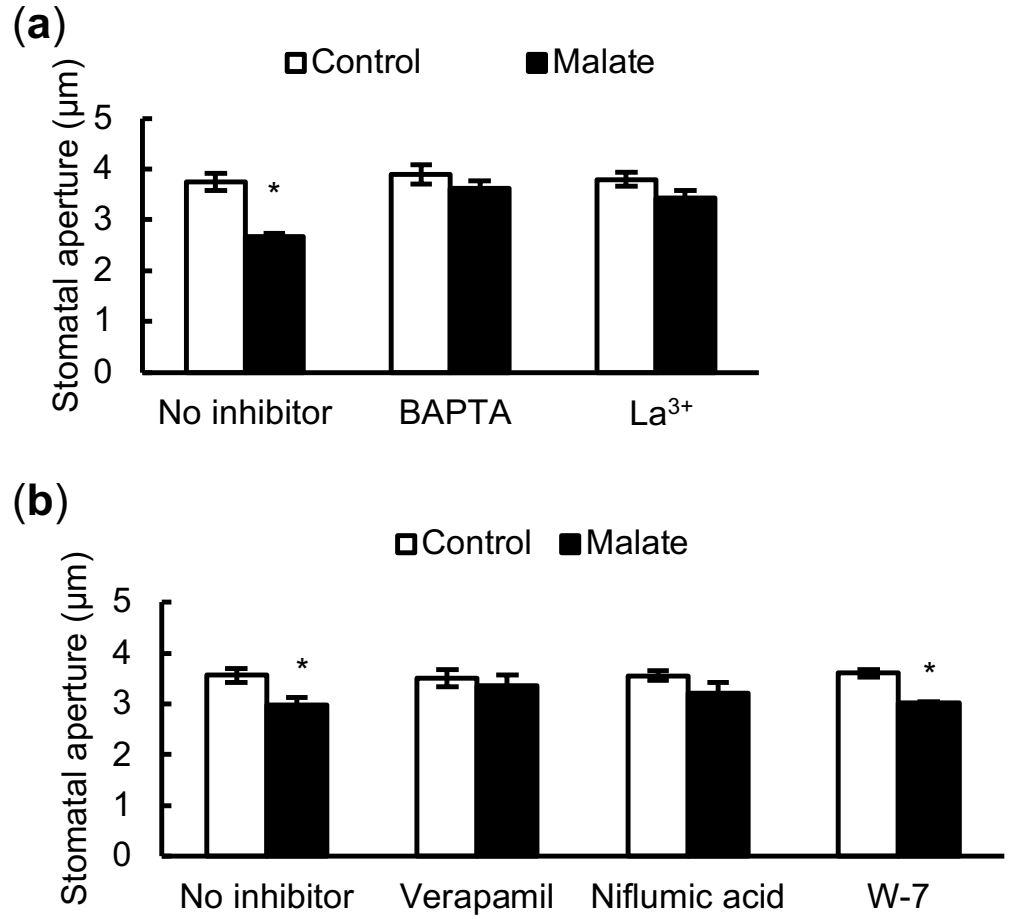

Fig 3.4. Malate-induced stomatal closure in the presence of Ca^{2+} channel blockers or Ca^{2+} chelators.

(a) Effects of 10 mM malate on stomatal aperture in the presence of 100 μM BAPTA or 5 mM $LaCl_3$ in wild-type plants. (b) Effects of 10 mM malate on stomatal aperture in the presence of 50 μM verapamil, 150 μM niflumic acid or 20 μM W7 in wild-type plants. Averages of stomatal apertures from at least three independent experiments (≥60 total stomata per bar) are shown. Data are mean ± SE. Asterisk denotes a significant difference vs. corresponding control ($P < 0.05$).

3.4.5. Malate-induced cytosolic Ca^{2+} elevation in guard cells

Treatment with a cytosolic Ca^{2+} chelator, BAPTA-AM completely suppressed the malate-induced stomatal closure (Fig. 3.5a), suggesting that the malate-induced stomatal closure requires elevation of $[Ca^{2+}]_{cyt}$. Perfusion of the bathing solution did not cause $[Ca^{2+}]_{cyt}$ elevation in the guard cells but perfusion with the bathing solution supplemented with malate caused $[Ca^{2+}]_{cyt}$ elevation (Fig. 3.5b). The treatment with malate significantly increased in frequency of the $[Ca^{2+}]_{cyt}$ elevation (Fig. 3.5c).

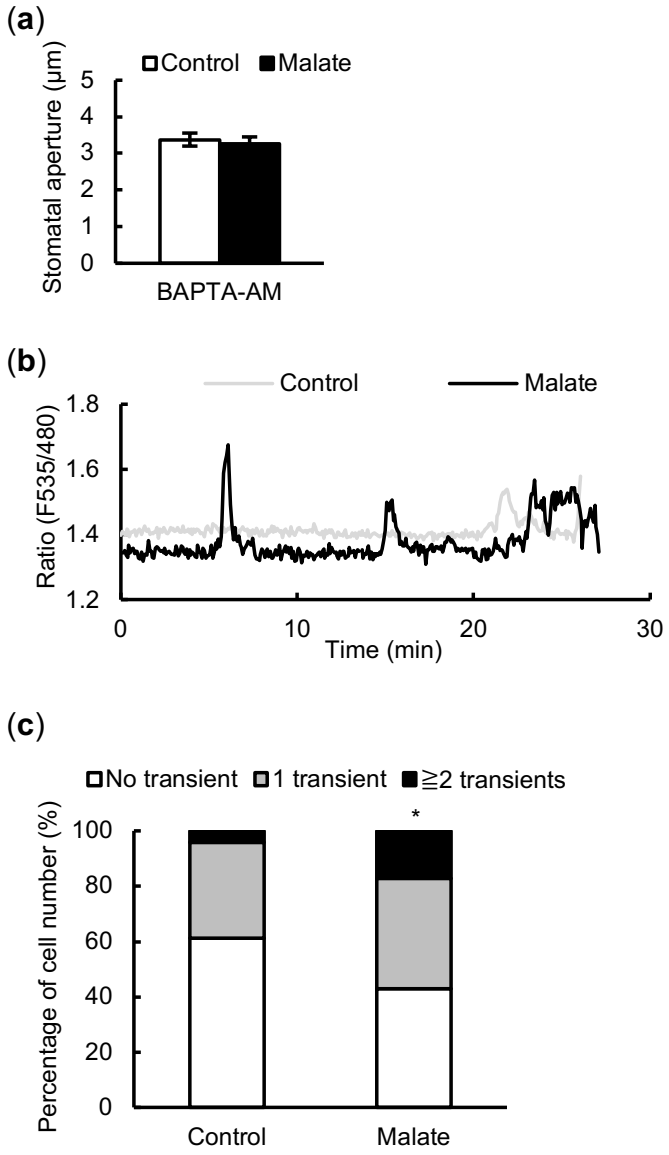

Fig 3.5. Malate-induced cytosolic Ca^{2+} elevation in guard cells.

(a) Effects of 10 mM malate on stomatal aperture in the presence of 25 μM BAPTA-AM in wild-type plants. (b) Representative traces of fluorescence emission ratios (535/480 nm) showing malate-induced transient $[Ca^{2+}]_{cyt}$ elevations in wild-type guard cells. The guard cells were treated by 10 mM malate 5 min and 10 mM $CaCl_2$ 20 min after the measurement. (c) Percentage of number of guard cells showing different number of transient $[Ca^{2+}]_{cyt}$ elevations. $[Ca^{2+}]_{cyt}$ elevations of 35–49 guard cells were counted when changes in fluorescence ratios were more than or equal to 0.1 U from the baseline ratio. Statistical differences were determined by χ^2 test, $^*P < 0.05$.

3.5. Discussion

Protein kinases activate anion channels in stomatal closure signaling (Mori *et al*., 2006; Brandt *et al*., 2015; Hua *et al*., 2012). Malate-induced stomatal closure was inhibited by the broad protein kinase inhibitor K252a (Fig 3.1a). This result indicates that protein kinases are also involved in the malate-induced stomatal closure. I examined the stomatal response of mutants of protein kinases which activate S-type anion channels and identified GHR1 as the protein kinase involved in malate-induced stomatal closure (Fig 3.1b). The activity of GHR1 is regulated by ABI2 in ABA signaling (Hua *et al*., 2012) and by HT1 in CO_2 signaling (Hõrak *et al*., 2016). However, the mutations in ABI2 or HT1 did not impair malate-induced stomatal closure (Fig 3.1b, 3.2). The pathway by which malate regulates the activity of GHR1 must be different from that of ABA and CO_2 signaling but malate would regulate anion channels *via* GHR1-dependent manner. Note that the malate-induced stomatal closure was not affected in the ABA-insensitive mutants, *pyr1 pyl1 pyl2 pyl4 pyl5 pyl8*, *abi1-1C*, and *abi2-1C* (Fig 3.2), indicating that the effect of malate is not attributed to increasing endogenous ABA.

ROS function upstream of GHR1 and produced by peroxidases or NAD(P)H oxidases (Pei *et al*., 2000; Mori *et al*., 2001; Hua *et al*., 2012). Malate induced ROS production in guard cells (Fig 3.3a). I also found that the malate-induced stomatal closure was inhibited by the peroxidase inhibitor SHAM but not either by the NAD(P)H oxidase inhibitor DPI or by the disruption of NAD(P)H oxidases RBOHD and RBOHF (Fig 3.3b, 3.3c). Therefore, malate should regulate the activity of GHR1 through ROS production catalyzed by SHAM-sensitive peroxidases in guard cells. Gross *et al*. suggested that malate dehydrogenases bound to the cell wall catalyze malate to generate NADH and in turn peroxidases bound to the cell wall catalyze NADH to produce ROS based on *in vitro* experiments (Gross *et al*., 1977). Consistent with their speculation, I demonstrated that malate actually induced ROS production *in planta*.

Ca^{2+} channels are activated by apoplastic ROS (Pei *et al*., 2000). The malate-induced stomatal closure was impaired by the extracellular Ca^{2+} chelator BAPTA or the Ca^{2+} channel blockers La^{3+}, verapamil, and niflumic acid (Fig 3.4a, 3.4b). The elevation of $[Ca^{2+}]_{cyt}$ leads to activation of S-type anion channels (Keller et al., 1989; Brandt et al., 2015). The cytosolic Ca^{2+} chelator BAPTA-AM completely inhibited the malate-induced stomatal closure (Fig 3.5a). In addition, malate actually caused $[Ca^{2+}]_{cyt}$ elevation in the guard cells (Fig 3.5b, 3.5c). These results indicate that the malate-induced stomatal closure is accompanied by the $[Ca^{2+}]_{cyt}$ elevation and that malate triggers the signal transduction that leads to the $[Ca^{2+}]_{cyt}$ elevation in the guard cells. However, the malate-induced stomatal closure was not impaired by the disruption of both CPK3 and CPK6 (Fig 3.1b) or by a CaM antagonist W7 (Fig 3.4b). Malate may induce stomatal closure *via* Ca^{2+}-dependent pathway mediated by unknown W7-insensitive Ca^{2+} sensors.

Based on the present study, I proposed the model of guard-cell malate signaling. Malate promotes ROS production catalyzed by SHAM-sensitive peroxidases. ROS activate Ca^{2+} channels in a GHR1-dependent manner. This results in the elevation of $[Ca^{2+}]_{cyt}$ and the activation of Ca^{2+}-dependent activated protein kinases. GHR1 and/or Ca^{2+}-dependent activated protein kinases activate anion channels and thereby promote stomatal closure.

Summary

Previous reports showed that plants secrete malate under stress conditions and advocated that malate is a chemical signal of stomatal closure. However, other molecular mechanism of the malate-induced stomatal closure is unknown. In CHAPTER2, I addressed questions if malate modulates guard-cell anion channels. I demonstrated that malate directly activates an S-type anion channel SLAC1 essential for stomatal closure and the malate activation of SLAC1 requires the phosphorylation of SLAC1 by protein kinases. In CHAPTER3, I addressed questions how malate regulates stomatal closure signaling and leads to the phosphorylation of SLAC1. I demonstrated that the malate signal is mediated by a signaling component GHR1 and second messengers ROS and Ca^{2+}. My results revealed that extracellular malate activates SLAC1, and that malate induces stomatal closure *via* a GHR1- and ROS-dependent pathway that stimulates Ca^{2+} signaling in guard cells (Fig 4.1). These results indicates that malate functions as a signaling molecule in the stomatal movement in *Arabidopsis thaliana*.

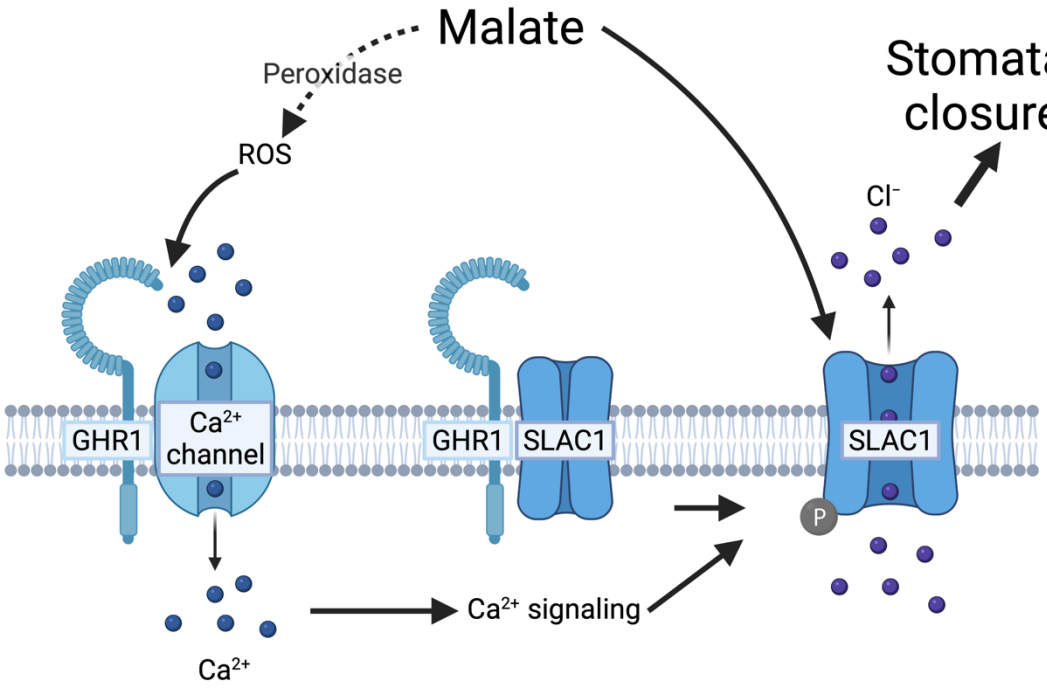

Fig 4.1. A proposed model of malate-induced stomatal closure in Arabidopsis guard cells.

Created with BioRender.com.

Acknowledgements

I am deeply grateful to Dr. Yoshiyuki Murata for his firm guidance, continuous encouragement, and valuable suggestion throughout the course of this study and making my university life irreplaceable.

I am grateful to Dr. Yoshimasa Nakamura, Dr. Shintaro Munemasa and Dr. Toshiyuki Nakamura for their valuable advice and useful suggestions throughout the course of this study.

I am grateful to Dr. Yoshinobu Kimura for his valuable comments and constructive suggestions.

I am grateful to Dr. Izumi C. Mori and Dr. Eiji Okuma for their experimental discussions.

Finally, I thank all other members of both laboratory of Chemistry of Bio-signaling and laboratory of Food Biochemistry for their discussion.

References

Acharya BR, Jeon BW, Zhang W *et al*. 2013. Open Stomata 1 (OST1) is limiting in abscisic acid responses of Arabidopsis guard cells. *New Phytol* **200**: 1049–63

Allaway WG. 1973. Accumulation of malate in guard cells of *Vicia faba* during stomatal opening. *Planta* **110**: 63–70

Allen GJ, Kwak JM, Chu SP, Llopis J, Tsien RY, Harper JF, Schroeder JI. 1999. Cameleon calcium indicator reports cytoplasmic calcium dynamics in *Arabidopsis* guard cells. *Plant Journal* **19**: 735–747

Araújo WL, Nunes-Nesi A, Osorio S, Usadel B, Fuentes D, Nagy R, Balbo I, Lehmann M, Studart-Witkowski C, Tohge T *et al.* 2011. Antisense inhibition of the iron-sulphur subunit of succinate dehydrogenase enhances photosynthesis and growth in tomato via an organic acid-mediated effect on stomatal aperture. *Plant Cell* **23**: 600–627

Batistič O, Sorek N, Schültke S, Yalovsky S, Kudla J 2008. Dual Fatty Acyl Modification Determines the Localization and Plasma Membrane Targeting of CBL/CIPK Ca^{2+} Signaling Complexes in *Arabidopsis*. *Plant Cell* **20**: 1346–1362

Bolwell GP, Bindschedler LV, Blee KA *et al*. 2002. The apoplastic oxidative burst in response to biotic stress in plants: a three-component system. *J Exp Bot* **53**: 1367–76

Brandt B, Brodsky DE, Xue S, Negi J, Iba K, Kangasjärvi J, Ghassemian M, Stephan AB, Hu H, Schroeder JI. 2012. Reconstitution of abscisic acid activation of SLAC1 anion channel by CPK6 and OST1 kinases and branched ABI1 PP2C phosphatase action. *Proceedings of the National Academy of Sciences, USA* **109**: 10593–10598

Brandt B, Munemasa S, Wang C, Nguyem D, Yong T, Yang PG, Poretsky E, Belknap TF, Waadt R, Alemán F *et al.* 2015. Calcium specificity signaling mechanisms in abscisic acid signal transduction in Arabidopsis guard cells. *eLife* **4**: e03599

Chen Y, Hu L, Punta M, Bruni R, Hillerich B, Kloss B, Rost B, Love J, Siegelbaum SA, Hendrickson WA. 2010. Homologue structure of the SLAC1 anion channel for closing stomata in leaves. *Nature* **467**: 1074–1080

Cubero-Font P, Maierhofer T, Jaslan J, Rosales MA, Espartero J, Díaz-Rueda P, Müller HM, Hürter AL, Al-Rasheid KAS, Marten I *et al.* 2016. Silent S-Type Anion Channel Subunit SLAH1 Gates SLAH3 Open for Chloride Root-to-Shoot Translocation. *Current Biology* **26**: 2213–2220

Cutler SR, Rodriguez PL, Finkelstein RR *et al*. 2010. Abscisic Acid: Emergence of a Core Signaling Network. *Annu Rev Plant Biol* **61**: 651–79

Daloso DM, Antunes WC, Pinheiro DP *et al*. 2015. Tobacco guard cells fix CO_2 by both Rubisco and PEPcase while sucrose acts as a substrate during light-induced stomatal opening. *Plant Cell Environ* **38**: 2353–71

Daloso DM, Medeiros DB, Anjos LD, Yoshida T, Araújo WL, Fernie AR. 2017. Metabolism within the specialized guard cells of plants. *New Phytologists* **216**: 1018–1033

Delhaize E, Ryan PR. 1995. Aluminum Toxicity and Tolerance in Plants. *Plant Physiol* **107**: 315–321

Deng Y-N, Kashtoh H, Wang Q, Zhen G-X, Li Q-Y, Tang L-H, Gao H-L, Zhang C-R, Qin L, Su M *et al.* 2021. Structure and activity of SLAC1 channels for stomatal signaling in leaves. *Proceedings of the National Academy of Sciences, USA* 118: e2015151118

Dittrich P, Raschke K. 1977. Malate metabolism in isolated epidermis of *Commelina communis* L. in relation to stomatal functioning. *Planta* **134**: 77–81

Engineer CB, Hashimoto-Sugimoto M, Negi J *et al*. 2016. CO_2 Sensing and CO_2 Regulation of Stomatal Conductance: Advances and Open Questions. *Trends Plant Sci* **21**: 16–30

Fernie AR, Martinoia E. 2009. Malate. Jack of all trades or master of a few? *Phytochemistry* **70**: 828–832

Fujii Y, Kodama Y. 2015. In planta comparative analysis of improved green fluorescent proteins with reference to fluorescence intensity and bimolecular fluorescence complementation ability. *Plant Biotechnology* **32**: 81–87

Fujita T, Noguchi K, Terashima I. 2013. Apoplastic mesophyll signals induce rapid stomatal responses to CO_2 in *Commelina communis*. *New Phytologist* **199**: 395–406

Gabriel R, Kesselmeier J. 1999. Apoplastic Solute Concentrations of Organic Acids and Mineral Nutrients in the Leaves of Several Fagaceae. *Plant Cell Physiology* **40**: 604–612

Geiger D, Scherzer S, Mumm P, Stange A, Marten I, Bauer H, Ache P, Matschi S, Liese A, Al-Rasheid KAS *et al.* 2009. Activity of guard cell anion channel SLAC1 is controlled by drought-stress signaling kinase-phosphatase pair. *Proceedings of the National Academy of Sciences, USA* **106**: 21425–21430

Geiger D, Maierhofer T, Al-Rasheid KAS, Scherzer S, Mumm P, Liese A, Ache P, Wellmann C, Marten I, Grill E *et al.* 2011. Stomatal closure by fast abscisic acid signaling is mediated by the guard cell anion channel SLAH3 and the receptor RCAR1. *Science Signaling* **4**: ra32

Gonzalez-Guzman M, Pizzio GA, Antoni R *et al*. 2012. *Arabidopsis* PYR/PYL/RCAR Receptors Play a Major Role in Quantitative Regulation of Stomatal Aperture and Transcriptional Response to Abscisic Acid. *Plant Cell* **24**: 2483–96

Gross GG, Janse C, Elstner EF. 1977. Involvement of Malate, Monophenols, and the Superoxide Radical in Hydrogen Peroxide Formation by Isolated Cell Walls from Horseradish (*Armoracia lapathijolia* Gilib.) *Planta* **136**: 271–6

Han J-P, Köster P, Drerup MM *et al*. 2019. Fine-tuning of RBOHF activity is achieved

by differential phosphorylation and Ca^{2+} binding. *New Phytol* **221**: 1935–49

Hashimoto-Sugimoto M, Negi J, Monda K *et al*. 2016. Dominant and recessive mutations in the Raf-like kinase *HT1* gene completely disrupt stomatal responses to CO_2 in Arabidopsis. *J Exp Bot* **67**: 3251–61

Hedrich R, Busch H, Raschke K. 1990. Ca^{2+} and nucleotide dependent regulation of voltage dependent anion channels in the plasma membrane of guard cells. *EMBO Journal* **9**: 3889–3892

Hedrich R, Marten I. 1993. Malate-induced feedback regulation of plasma membrane anion channels could provide a CO_2 sensor to guard cells. *EMBO Journal* **12**: 897–901

Hedrich R, Marten I, Lohse G, Dietrich P, Winter H, Lohaus G, Heldt H-W. 1994. Malate-sensitive anion channels enable guard cells to sense changes in the ambient CO_2 concentration. *Plant Journal* **6**: 741–748

Hedrich R, Neimanis S, Savchenko G, Felle HH, Kaise WM, Heber U. 2001. Changes in apoplastic pH and membrane potential in leaves in relation to stomatal responses to CO_2, malate, abscisic acid or interruption of water supply. *Planta* **213**: 594–601

Hedrich R. 2012. Ion channels in plants. *Physiological Reviews* **92**: 1777–1811

Hetherington AM, Woodward FI. 2003. The role of stomata in sensing and driving environmental change. *Nature* **423**: 901–908

Hiyama A, Takemiya A, Munemasa S *et al*. 2017. Blue light and CO_2 signals converge to regulate light-induced stomatal opening. *Nat Commun* **8**: 1284

Hõrak H, Sierla M, Tõldsepp K *et al*. 2016. A Dominant Mutation in the HT1 Kinase Uncovers Roles of MAP Kinases and GHR1 in CO_2-Induced Stomatal Closure. *Plant Cell* **28**: 2493–509

Hua D, Wang C, He J *et al*. 2012. A Plasma Membrane Receptor Kinase, GHR1, Mediates Abscisic Acid- and Hydrogen Peroxide-Regulated Stomatal Movement in

Arabidopsis. *Plant Cell* **24**: 2546–61

Huang S, Waadt R, Nuhkat M, Kollist H, Hedrich R, Roelfsema MRG. 2019. Calcium signals in guard cells enhance the efficiency by which abscisic acid triggers stomatal closure. *New Phytologist* **224**: 177–187

Hubbard KE, Nishimura N, Hitomi K *et al*. 2010. Early abscisic acid signal transduction mechanisms: newly discovered components and newly emerging questions. *Genes Dev* **24**: 1695–708

Jumper J, Evans R, Pritzel A *et al*. 2010. Highly accurate protein structure prediction with AlphaFold. *Nature* 596: 583–589

Keller BU, Hedrich R, Raschke K. 1989. Voltage-dependent anion channels in the plasma membrane of guard cells. *Nature* **341**: 450–453

Khokon MAR, Okuma E, Hossain MA *et al*. 2011. Involvement of extracellular oxidative burst in salicylic acid-induced stomatal closure in *Arabidopsis*. *Plant Cell Environ* **34**: 434–43

Khokon MAR, Salam MA, Jammes F *et al*. 2017. MPK9 and MPK12 function in SA-induced stomatal closure in *Arabidopsis thaliana*. *Biosci Biotechnol Biochem* **81**: 1394–400

Kollist H, Jossier M, Laanemets K *et al*. 2011. Anion channels in plant cells. *FEBS J* **278**:4277–92

Kondo N, Maruta I. 1987. Abscisic acid-induced stomatal closure in *Vicia faba* epidermal strip. Excretion of solutes from guard cells and increase in elastic modulus of guard cell wall. *Plant Cell Physiology* **28**: 355–364

Konrad KR, Hedrich R. 2008. The use of voltage-sensitive dyes to monitor signal-induced changes in membrane potential-ABA triggered membrane depolarization in guard cells. *Plant Journal* **55**: 161–173

Kwak JM, Mori IC, Pei Z-M *et al*. 2003. NADPH oxidase *AtrbohD* and *AtrbohF* genes

function in ROS-dependent ABA signaling in *Arabidopsis*. *EMBO J* **22**: 2623–33

Lee M, Choi Y, Burla B, Kim Y-Y, Jeon B, Maeshima M, Yoo J-Y, Martinoia E, Lee Y. 2008. The ABC transporter AtABCB14 is a malate importer and modulates stomatal response to CO_2. *Nature Cell Biology* **10**: 1217–1223

Lee SC, Lan W, Buchanan BB, Luan S. 2009. A protein kinase-phosphatase pair interacts with an ion channel to regulate ABA signaling in plant guard cells. *Proceedings of the National Academy of Sciences, USA* **106**: 21419–21424

Linder B, Raschke K. 1992. A slow anion channel in guard cells, activating at large hyperpolarization, may be principal for stomatal closing. *FEBS Letter* **16**: 27–30

Maierhofer T, Diekmann M, Offenborn JN, Lind C, Bauer H, Hashimoto K, Al-Rasheid KAS, Luan S, Kudla J, Geiger D *et al.* 2014. Site- and kinase-specific phosphorylation-mediated activation of SLAC1, a guard cell anion channel stimulated by abscisic acid. *Science Signaling* **7**: ra86

Mayer ML, Westbrook GL, Guthrie PB. 1984. Voltage-dependent block by Mg^{2+} of NMDA responses in spinal cord neurones. *Nature* **309**: 261–263

Melotto M, Underwood W, He SY. 2008. Role of Stomata in Plant Innate Immunity and Foliar Bacterial Diseases. *Annu Rev Phytopathol* **46**: 101-122

Meyer S, Mumm P, Imes D, Endler A, Weder B, Al-Rasheid KAS, Geiger D, Marten I, Martinoia E, Hedrich R. 2010. *At*ALMT12 represents an R-type anion channel required for stomatal movement in Arabidopsis guard cells. *Plant Journal* **63**: 1054–1062

Mori IC, Pinontoan R, Kawano T *et al*. 2001. Involvement of superoxide generation in salicylic acid-induced stomatal closure in *Vicia faba*. *Plant Cell Physiol* **42**: 1383–8

Mori IC, Murata Y, Yang Y, Munemasa S, Wang Y-F, Andreoli S, Tiriac H, Alonso JM, Harper JF, Ecker JR *et al.* 2006. CDPKs CPK6 and CPK3 function in ABA regulation of guard cell S-type anion- and Ca^{2+}-permeable channels and stomatal

closure. *PLoS Biology* **10**: e327

Munemasa S, Hossain MA, Nakamura Y *et al*. 2011. The Arabidopsis Calcium-Dependent Protein Kinase, CPK6, Functions as a Positive Regulator of Methyl Jasmonate Signaling in Guard Cells. *Plant Physiol* **155**: 553–61

Munemasa S, Hauser F, Park J *et al*. 2015. Mechanisms of abscisic acid-mediated control of stomatal aperture. *Curr Opin Plant Biol* **28**: 154–62

Munemasa S, Hirao Y, Tanami K, Mimata Y, Nakamura Y, Murata Y. 2019. Ethylene Inhibits Methyl Jasmonate-Induced Stomatal Closure by Modulating Guard Cell Slow-Type Anion Channel Activity via the OPEN STOMATA 1/SnRK2.6 Kinase-Independent Pathway in Arabidopsis. *Plant Cell Physiology* **60**: 2263–2271

Murata Y, Mori IC, Munemasa S. 2015. Diverse Stomatal Signaling and the Signal Integration Mechanism. *Annu Rev Plant Biol* **66**: 369–92

Mustilli A-C, Merlot S, Vavasseur A, Fenzi F, Giraudat J. 2002. Arabidopsis OST1 protein kinase mediates the regulation of stomatal aperture by abscisic acid and acts upstream of reactive oxygen species production. *Plant Cell* **14**: 3089–3099

Negi J, Matsuda O, Nagasawa T, Oba Y, Takahashi H, Kawai-Yamada M, Uchimiya H, Hashimoto M, Iba K. 2008. CO_2 regulator SLAC1 and its homologues are essential for anion homeostasis in plant cells. *Nature* **452:** 483–486

Nishimura N, Yoshida T, Murayama M *et al*. 2004. Isolation and Characterization of Novel Mutants Affecting the Abscisic Acid Sensitivity of *Arabidopsis* Germination and Seedling Growth. *Plant Cell Physiol* **45**: 1485–99

Nour-Eldin HH, Hansen BG, Nørholm MHH, Jensen JK, Halkier BA. 2006. Advancing uracil-excision based cloning towards an ideal technique for cloning PCR fragments. *Nucleic Acids Research* **34**: e122

Nowak L, Bregestovski P, Ascher P, Herbet A, Prochiantz A. 1984. Magnesium gates glutamate-activated channels in mouse central neurones. *Nature* **307**: 462–465

Outlaw Jr. WH, Lowry OH. 1977. Organic acid and potassium accumulation in guard cells during stomatal opening. *Proceedings of the National Academy of Sciences, USA* **74**: 4434–4438

Qi Z, Stephens NR, Spalding EP. 2006. Calcium entry mediated by GLR3.3, an Arabidopsis glutamate receptor with a broad agonist profile. *Plant Physiology* **142**: 963–971

Pei Z-M, Murata Y, Benning G *et al*. 2000. Calcium channels activated by hydrogen peroxide mediate abscisic acid signalling in guard cells. *Nature* **406**: 731–4

Prodhan MY, Munemasa S, Nahar MNEN *et al*. 2018. Guard Cell Salicylic Acid Signaling Is Integrated into Abscisic Acid Signaling via the Ca^{2+}/CPK-Dependent Pathway. *Plant Physiol* **178**: 441–50

Raschke K, Schnabl H. 1978. Availability of Chloride Affects the Balance between Potassium Chloride and Potassium Malate in Guard Cells of *Vicia faba* L. *Plant Physiology* **62**: 84–87

Raschke K. 2003. Alternation of the slow with the quick anion conductance in whole guard cells effected by external malate. *Planta* **217**: 651–657

Robaina-Estévez S, Daloso DM, Zhang Y *et al*. 2017. Resolving the central metabolism of Arabidopsis guard cells. *Sci Rep* **7**: 8307

Sasaki T, Mori IC, Furuichi T, Munemasa S, Toyooka K, Matsuoka K, Murata Y, Yamamoto Y. 2010. Closing Plant Stomata Requires a Homolog of an Aluminum-Activated Malate Transporter. *Plant Cell Physiology* **51**: 354–365

Schmidt C, Schelle I, Liao YJ, Schroeder JI. 1995. Strong regulation of slow anion channels and abscisic acid signaling in guard cells by phosphorylation and dephosphorylation events. *Proceedings of the National Academy of Sciences, USA* **92**: 9535–9539

Schroeder JI, Hagiwara S. 1989. Cytosolic calcium regulates ion channels in the

plasma membrane of *Vicia faba* guard cells. *Nature* **338**: 427–430

Schroeder JI, Keller BU. 1992. Two types of anion channel currents in guard cells with distinct voltage regulation. *Proceedings of the National Academy of Sciences, USA* **89**: 5025–5029

Schroeder JI, Schmidt C, Sheaffer J. 1993. Identification of High-Affinity Slow Anion Channel Blockers and Evidence for Stomatal Regulation by Slow Anion Channels in Guard Cells. *Plant Cell* **5**: 1831–1841

Schroeder JI, Allen GJ, Hugouvieux V, Kwak JM, Waner D. 2001. Guard cell signal transduction. *Annual Review of Plant Physiology and Plant Molecular Biology* **52** : 627–58

Siegel RS, Xue S, Murata Y, Yang Y, Nishimura N, Wang A, Schroeder JI. 2009. Calcium elevation-dependent and attenuated resting calcium-dependent abscisic acid induction of stomatal closure and abscisic acid-induced enhancement of calcium sensitivities of S-type anion and inward-rectifying K^+ channels in Arabidopsis guard cells. *Plant Journal* **59**: 207–220

Sirichandra C, Gu D, Hu H-C *et al*. 2009. Phosphorylation of the Arabidopsis AtrbohF NADPH oxidase by OST1 protein kinase. *FEBS Lett* **583**: 2982–6

Sierla M, Hõrak H, Overmyer K *et al*. 2018. The Receptor-like Pseudokinase GHR1 Is Required for Stomatal Closure. *Plant Cell* **30**: 2813–37

Shimazaki K, Doi M, Assmann SM, Kinoshita T. 2007. Light regulation of stomatal movement. *Annu Rev Plant Biol* **58**: 219-247

Suhita D, Raghavendra AS, Kwak JM *et al*. 2004. Cytoplasmic Alkalization Precedes Reactive Oxygen Species Production during Methyl Jasmonate- and Abscisic Acid-Induced Stomatal Closure. *Plant Physiol* **134**: 1536–45

Umezawa T, Sugiyama N, Mizoguchi M *et al*. 2009. Type 2C protein phosphatases directly regulate abscisic acid-activated protein kinases in *Arabidopsis*. *Proc Natl*

Acad Sci USA **106**: 17588–93

Vahisalu T, Kollist H, Wand Y-F, Nishimura N, Chan W-Y, Valerio G, Lamminmäki A, Brosché M, Moldau H, Desikan R *et al.* 2008. SLAC1 is required for plant guard cell S-type anion channel function in stomatal signalling. *Nature* **452**: 487–491

Van Kirk CA, Raschke K. 1978a. Presence of Chloride Reduces Malate Production in Epidermis during Stomatal Opening. *Plant Physiology* **61**: 361–364

Van Kirk CA, Raschke K. 1978b. Release of Malate from Epidermal Strips during Stomatal Closure. *Plant Physiology* **61**: 474–475

Varadi M, Anyango S, Mandar D *et al*. 2021. AlphaFold Protein Structure Database: massively expanding the structural coverage of protein-sequence space with high-accuracy models. *Nucleic Acids Research* **50**: D439–D444

Vincill ED, Bieck AM, Spalding EP. 2012. Ca^{2+} conduction by an amino acid-gated ion channel related to glutamate receptors. *Plant Physiology* **159**: 40–46

Wang Y, Blatt MR. 2011. Anion channel sensitivity to cytosolic organic acids implicates a central role for oxaloacetate in integrating ion flux with metabolism in stomatal guard cells. *Biochemical Journal* **439**: 161–170

Wang C, Zhang J, Schroeder JI. 2017. Two-electrode Voltage-clamp Recordings in *Xenopus laevis* Oocytes: Reconstitution of Abscisic Acid Activation of SLAC1 Anion Channel via PYL9 ABA Receptor. *Bio-protocol* **7**: e2114

Wang C, Zhang J, Wu J, Brodsky DE, Schroeder JI. 2018. Cytosolic malate and oxaloacetate activate S-type anion channels in *Arabidopsis* guard cells. *New Phytologist* **220**: 178–186

Ye W, Munemasa S, Shinya T, Wu W, Ma T, Lu J, Kinoshita T, Kaku H, Shibuya N, Murata Y. 2020. Stomatal immunity against fungal invasion comprises not only chitin-induced stomatal closure but also chitosan-induced guard cell death. *Proceedings of the National Academy of Sciences, USA* **117**, 20932–20942

Yoshida R, Mori IC, Kamizono N, Shichiri Y, Shimatani T, Miyata F, Honda K, Iwai S.

2016. Glutamate functions in stomatal closure in *Arabidopsis* and fava bean. *Journal of Plant Research* **129**: 39–49